Nonlinear Dyn (2020) 100:3555–3573
https://doi.org/10.1007/s11071-020-05720-5

ORIGINAL PAPER

Multilayer neural networks-based control of underwater vehicles with uncertain dynamics and disturbances

Kairong Duan · Simon Fong · C. L. Philip Chen

Received: 17 December 2019 / Accepted: 21 May 2020 / Published online: 11 June 2020

Abstract In the presence of uncertain dynamic terms and external disturbances, the problem of trajectory tracking with application to an underactuated underwater vehicle is addressed in this paper. Based on Lyapunov theory and properties of neural networks, a nonlinear neural controller is designed, where multilayer neural networks are adopted to approximate the unmodeled dynamic terms and external disturbances. In order to confine the values of estimated weights within predefined bounds, smooth projection functions are employed. Moreover, measurement noises are considered so as to simulate realistic operation scenario, while filters are designed to get cleaner states. From the stability analysis, it is proven that the tracking errors are globally uniformly ultimately bounded. Numerical examples are provided to demonstrate the robustness of the controller in the presence of unmodeled terms, disturbances and measurement noises.

K. Duan (✉) · S. Fong · C. L. P. Chen
Faculty of Science and Technology, University of Macau, Taipa 999078, Macau, China
e-mail: yb67408@connect.um.edu.mo

C. L. P. Chen
School of Computer Science and Engineering, South China University of Technology, Guangzhou 510006, Guangdong, China

C. L. P. Chen
College of Navigation, Dalian Maritime University, Dalian 116026, China

Keywords Multilayer neural networks · Underwater vehicles · Unmodeled terms · Disturbances · Measurement noises

1 Introduction

In recent years, the control of autonomous underwater vehicles (AUVs) has received considerable attention in academic and engineering areas such as sampling, water quality monitoring, archaeological surveys and plume tracing [1–4], etc. Although much effort has been made toward different types of AUVs including surface vehicles [5, 6] and underwater vehicles [7–11], it is challenging to precisely steer an AUV along a reference trajectory due to the complex dynamics and uncertainties introduced by internal system and the external environment. Moreover, many of the AUVs have fewer inputs than degrees of freedom (DOF) which makes it more difficult to derive a control law. In this paper, we research for a solution that addresses the tracking problem for underactuated underwater vehicle in the presence of unmodeled dynamics and time-varying disturbances.

Conventional backstepping technique [12–14] is one of the most popular approaches to deal with the control problem of AUVs. For example, backstepping techniques [13] were used to derive the control law for an underactuated AUV in three-dimensional space,

and the proposed controller was able to guarantee the tracking error within an arbitrarily small neighborhood of zero. However, unknown dynamics and unpredictable disturbances were not considered. It should be noted that the presence of uncertainties that are induced by wind, waves or ocean currents can cause high-frequency uncertain dynamics, which consequently affect the performance of model-based controllers, leading to close-loop instability [15]. The backstepping technique was also reported in [12]. It was formulated from the derivation of control law, where the uncertainties and disturbances were estimated and compensated using an adaptive algorithm. However, fully actuated models rather than underactuated dynamics were used in the prior arts.

Other control approaches including linear proportional derivative (PD) [16], linear quadratic regulator (LQR) [17], model predictive control (MPC) [18, 19], adaptive control [20, 21], H_∞ [22] and sliding mode control (SMC) [23–25] have also been presented. Different types of uncertainties such as unmodeled dynamics of the tether [16, 19, 20], model parameter error [18], unknown hydrodynamic coefficient [26] and ocean current [27] were considered in the studies. In the Lyapunov-based MPC framework [18], online optimization was used to improve the trajectory tracking performance, but the magnitude of the disturbance caused by ocean current was assumed constant. By contrast, constant, sinusoidal and a period of disturbances were tested in [23]. Although specific dynamics of three DOF lateral AUVs were studied here, many works focused on model-free control schemes [16, 26, 28, 29]. For instance, based on completely unknown dynamic systems, reinforcement learning (RL) techniques were employed in [29], where the critic and action neural networks were designed to approximate an unknown long-term performance index and controller. Different from RL-based controller [29–31], disturbance observer (DOB)-based control methods do not have to use large feedback gains [32]. In [33], DOB was introduced to compensate the time-varying external disturbance for an unmanned surface vehicle. It is noted that the unmodeled dynamics was separately compensated by neural network minimum learning parameter method. Thus, it is more complicated than directly estimating both of the unmodeled terms and disturbances. Readers are also referred to [34–40] for other control methods like transverse function control, output feedback control, etc.

Research works which applied uniform approximation ability of fuzzy logic systems (FLSs) [26, 28, 41–44] and neural networks (NNs) [45–51], reported promising results on the control of AUVs. As the controllers in [26, 28] were designed with fully unknown parametric dynamics and uncertainties, fuzzy systems were used to approximate ideal backstepping control law and unknown lumped dynamics. When it comes to model-based control, FLSs can also be applied to estimate uncertainties in the model of surface vehicle [41], underwater vehicle [42], uncertain high-order nonlinear systems [43] or multi-input and multi-output (MIMO) nonlinear systems [44]. Single-layer NNs were applied to compensate the unmodeled terms and external time-varying unmodeled forces and moments in [45, 46, 51]. Multilayer NNs were explored in [47, 48] as a solution for accomplishing the compensation. However, both of two tracking errors were semi-globally uniformly ultimately bounded (SGUUB). Namely, the stability can only be achieved within a certain region. In addition, neither of them can guarantee the weights of multilayer NNs to be bounded. A neural network-based target tracking controller and a saturated trajectory tracking controller were proposed, respectively, in [49, 50]. MATLAB simulations and comparative studies were provided to validate the efficacy of the proposed theoretical results therein. However, in [49], the kinematic model for altitude was simplified, and only 5-DOF was considered. On the other hand, in [50], the authors chose fully actuated underwater vehicle model as their study model, which cannot be applied to control underactuated underwater vehicles. In [52], a recurrent neural network with convolution was proposed for unmanned underwater vehicle online obstacle avoidance on the vertical plane. The model was simplified by ignoring the heave, roll and pitch motions. Moreover, hybrid fuzzy neural-network-based controller was established in [53, 54]. Nevertheless, all these aforementioned studies do not consider the measurement noises that inevitably would have existed in the process of sensing data.

Motivated by the above-mentioned significant research works and detailed discussions, the main contribution of this paper is threefold:

(1) A nonlinear smooth switching function-based multilayer NNs tracking controller is designed for an underactuated underwater vehicle, where a regular multilayer NNs controller works within the NNs active region, while a robust controller works outside the NNs active region. Through Lyapunov stability analysis, the globally uniformly ultimately bounded is guaranteed, while the controllers proposed in [16, 17, 47, 48] can only obtain local stability and semi-globally uniformly ultimately bounded, respectively.
(2) Uncertain dynamic terms and external time-varying disturbances induced by wind, waves and currents are considered and estimated by multilayer NNs. Unlike the constant assumption of the disturbances in [18, 55], we consider complicated but more realistic time variant disturbances. Compared with the conventional single-layer NNs [51] and multilayer NNs [47, 48], in this paper smooth projections are introduced to limit the estimated weights remaining within predefined bounds.
(3) Measurement noises are considered to simulate a more realistic application scenario. To clean the measured states, noise filters are designed. By contrast, none of [41–51] takes into account the harmful effects of measurement noises.

In summary, a multilayer NN-based tracking controller, that can meet multiple requirements including globally uniformly ultimately bounded of the closed-loop system, disturbance rejection ability and robustness to measurement noises, is proposed.

The rest of the paper is organized as follows: Sect. 2 introduces notations, vehicle models, neural networks and the control objective. Section 3 gives the details of controller design. Section 4 presents numerical examples. Section 5 concludes the work of this paper and describes the future work.

2 Problem formulation

2.1 Notation

Throughout the paper, the transpose operation for a given matrix $\mathbf{a} \in \mathbb{R}^{m\times n}$ is denoted by $\mathbf{a}^\top \in \mathbb{R}^{n\times m}$. The Euclidean norm applying on a vector $\mathbf{b} \in \mathbb{R}^m$ is denoted by $\|\mathbf{b}\| = \sqrt{\mathbf{b}^\top \mathbf{b}}$, with $\mathbb{R}^m$ representing m-dimensional Euclidean space. For a n-by-n square matrix $\mathbf{c}$, the *trace* is defined to be the sum of the elements on the main diagonal, specified as

$$\mathrm{tr}(\mathbf{c}) = \sum_{i=1}^{n} c_{ii} = c_{11} + c_{22} + \cdots + c_{nn}$$

where c_{ii} denotes the entry on the ith row and ith column of matrix $\mathbf{c}$. The Frobenius norm is defined as the square root of the sum of the absolute squares of its elements:

$$\|\mathbf{c}\|_{\mathrm{F}} = \sqrt{\sum_{i=1}^{m}\sum_{j=1}^{n} |c_{ij}|^2}$$

where c_{ij} is the entry on the ith row and ith column of matrix $\mathbf{c}$, with the following property:

$$\mathrm{tr}(\mathbf{c}^\top \mathbf{c}) = \|\mathbf{c}\|_{\mathrm{F}}^2.$$

In addition, the symbols that are used in this paper are described in Table 1.

2.2 Mathematical modeling of AUVs

2.2.1 Kinematic equations

Considering an underactuated underwater vehicle, we first introduce a global coordinate frame $\{U\}$ and a body frame $\{B\}$. The origin of each frame is located at the gravity center of a vehicle. Following [56], the kinematic equations of the vehicle can be written as

$$\begin{aligned} \dot{\boldsymbol{\eta}}_1 &= \mathbf{J}(\boldsymbol{\eta}_2)\boldsymbol{v}_1 \\ \dot{\mathbf{J}}(\boldsymbol{\eta}_2) &= \mathbf{J}(\boldsymbol{\eta}_2)\mathbf{S}(\boldsymbol{v}_2) \end{aligned} \tag{1}$$

where $\boldsymbol{\eta}_1 \in \mathbb{R}^3$ denotes the position of the gravity center. $\boldsymbol{v}_1, \boldsymbol{v}_2 \in \mathbb{R}^3$ are the linear velocity and angular velocity, respectively. $\mathbf{J}(\boldsymbol{\eta}_2)$ is the rotation matrix from $\{B\}$ to $\{U\}$. $\mathbf{S}(\cdot)$ is a skew-symmetric matrix which is given by

$$\mathbf{S}(\boldsymbol{\lambda}) = \begin{bmatrix} 0 & -\lambda_3 & \lambda_2 \\ \lambda_3 & 0 & -\lambda_1 \\ -\lambda_2 & \lambda_1 & 0 \end{bmatrix}$$

with the following properties

$$\mathbf{b}_1^\top \mathbf{S}(\mathbf{b}_2)\mathbf{b}_1 = 0 \tag{2}$$

and

Table 1 Descriptions of symbols

Symbol	Description	Symbol	Description
$\boldsymbol{\eta}_1$	Position	$\boldsymbol{\eta}_\mathrm{d}$	Desired trajectory
$\boldsymbol{v}_1$	Linear velocity	$\boldsymbol{v}_2$	Angular velocity
$\mathbf{J}(\boldsymbol{\eta}_2)$	Rotation matrix	$\mathbf{S}(\cdot)$	Skew-symmetric matrix
$\mathbf{M}_{\mathrm{RB}}$	Rigid-body mass matrix	$\mathbf{M}_\mathrm{A}$	Added mass matrix
$\mathbf{I}_{\mathrm{RB}}$	Rigid-body inertia matrix	$\mathbf{I}_\mathrm{A}$	Added inertia matrix
$\mathbf{T}$	Thrust force input	$\boldsymbol{\tau}$	Torque input
b	Buoyant force	mg	Gravitational force
$\mathbf{u}_x$	Unit vector $[1, 0, 0]^\top$	$\mathbf{u}_y$	Unit vector $[0, 1, 0]^\top$
$\mathbf{u}_z$	Unit vector $[0, 0, 1]^\top$	$\mathbf{W}$, $\mathbf{V}$	Weight matrix
$\mathbf{e}_i$	Error terms, $i = 1, 2, 3$	λ_i	Control gains, $i = 1, 2, 3$

$$\mathbf{S}(\mathbf{b}_1)\mathbf{b}_2 = -\mathbf{S}(\mathbf{b}_2)\mathbf{b}_1 \tag{3}$$

where $\mathbf{b}_1, \mathbf{b}_2 \in \mathbb{R}^3$.

Assumption 1 For a specific vehicle, its linear and angular velocities are always bounded, denoted as

$$||\boldsymbol{v}_1|| \leq v_{1\max}, \ ||\boldsymbol{v}_2|| \leq v_{2\max}$$

where $v_{1\max}$, $v_{2\max}$ are known positive values.

2.2.2 *Dynamic equations*

The dynamic equations of the underactuated vehicle are considered as

$$\begin{aligned} \mathbf{M}\dot{\boldsymbol{v}}_1 &= -\mathbf{S}(\boldsymbol{v}_2)\mathbf{M}\boldsymbol{v}_1 + \mathbf{n}_{v_1}\mathbf{T} + \mathbf{J}(\boldsymbol{v}_2)^\top(b - \mathrm{mg})\mathbf{u}_z + \mathbf{d}_{v_1} \\ \mathbf{I}\dot{\boldsymbol{v}}_2 &= \boldsymbol{\tau} + \mathbf{d}_{v_2} \end{aligned} \tag{4}$$

where $\mathbf{n}_{v_1} = [\mathbf{u}_x, \mathbf{u}_z]$, $\mathbf{M} = \mathbf{M}_{\mathrm{RB}} + \mathbf{M}_\mathrm{A} \in \mathbb{R}^{3\times3}$ and $\mathbf{I} = \mathbf{I}_{\mathrm{RB}} + \mathbf{I}_\mathrm{A} \in \mathbb{R}^{3\times3}$ represent constant symmetric positive definite mass and inertia matrices, respectively. $\mathbf{M}_{\mathrm{RB}} = \mathrm{diag}(m, m, m)$ and $\mathbf{M}_A = \mathrm{diag}(-X_{\dot{u}}, -Y_{\dot{v}}, -Z_{\dot{w}})$ are rigid-body mass matrix and added mass matrix, respectively. $\mathbf{I}_{\mathrm{RB}} = \mathrm{diag}(I_x, I_y, I_z)$ and $\mathbf{I}_\mathrm{A} = \mathrm{diag}(-L_{\dot{p}}, -M_{\dot{q}}, -N_{\dot{r}})$ denote rigid-body and added inertia matrix, respectively. $\mathbf{T} = [T_x, T_z]$, $\boldsymbol{\tau} = [\tau_x, \tau_y, \tau_z]^\top$ are control inputs. Let b be the buoyant force, mg be the gravitational force and $\mathbf{d}_{v_1}$, $\mathbf{d}_{v_2}$ be lumped unknown terms including unmodeled dynamic terms and external time-varying disturbances. Figure 1 illustrates the vehicle model in three-dimensional space. The rotations about x_b-axis, y_b-axis and z_b-axis are represented by *roll*, *pitch* and *yaw*.

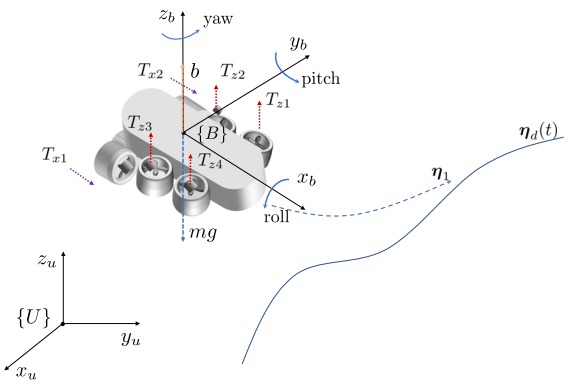

Fig. 1 Trajectory tracking of an underactuated underwater vehicle. The forces in x_b and z_b directions are represented by $T_x = T_{x1} + T_{x2}$ and $T_z = T_{z1} + T_{z2} + T_{z3} + T_{z4}$, respectively

Assumption 2 The lumped unknown terms and their derivatives are bounded, given as

$$\|\mathbf{d}_{v_1}\| + \|\dot{\mathbf{d}}_{v_1}\| \leq \zeta_1, \ \|\mathbf{d}_{v_2}\| + \|\dot{\mathbf{d}}_{v_2}\| \leq \zeta_2$$

where ζ_1, ζ_2 stand for known positive constants.

2.3 Multilayer neural networks

We first define a typical three-layer neural network structure in Fig. 2. The output of the three-layer NN is given as [57]

$$y_i = \sum_{j=1}^{N_2}\left[w_{ij}\sigma\Big(\sum_{k=1}^{N_1} v_{jk}x_k + \theta_{vj}\Big) + \theta_{wi}\right], \ i = 1, 2, \ldots, N_3 \tag{5}$$

where N_1, N_2 and N_3 denote the numbers of neurons in input layer, hidden layer and output layer,

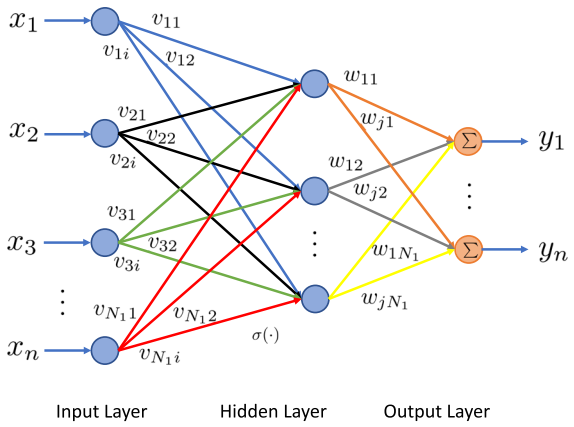

Fig. 2 The structure of the three-layer neural network

respectively. $\sigma(\cdot)$ is the activation function, which can be chosen as sigmoid function $1/(1+\mathrm{e}^{-\alpha z})$, hyperbolic function $\tanh(z)$, radial basis function $\mathrm{e}^{-(z-\mu)^2/c^2}$, etc. v_{jk} and w_{ij} are the first-to-second layer interconnection weights and the second-to-third layer interconnection weights, respectively. θ_{vj} and θ_{wi} are threshold offsets. Rewriting (5) in a compact form as

$$\mathbf{y} = \mathbf{W}^\top \sigma(\mathbf{V}^\top \mathbf{x}) \tag{6}$$

where $\mathbf{x} = [1, x_1, x_2, \ldots, x_{N_1}]^\top$, $\mathbf{y} = [y_1, y_2, \ldots, y_{N_3}]^\top$, and weight matrices $\mathbf{W}^\top \in \mathbb{R}^{N_3 \times (N_2+1)}$, $\mathbf{V}^\top \in \mathbb{R}^{N_2 \times (N_1+1)}$ contain all the elements w_{ij} and v_{jk}, respectively. It should be noted that θ_{vj}, θ_{wi} are included by assigning one as the first term in the vector $\sigma(\mathbf{V}^\top \mathbf{x})$. For a general function $\mathbf{f}(\mathbf{x}) : \mathbb{R}^n \to \mathbb{R}^m$, it can be approximated by

$$\mathbf{f}(\mathbf{x}) = \mathbf{W}^\top \sigma(\mathbf{V}^\top \mathbf{x}) + \boldsymbol{\epsilon}(\mathbf{x}) \tag{7}$$

where $\boldsymbol{\epsilon}(\mathbf{x})$ is a neural network functional reconstruction error vector, satisfying $\|\boldsymbol{\epsilon}(\mathbf{x})\| \le \epsilon_{\max}$, and $\epsilon_{\max}$ is a positive number; $\mathbf{x}$ and $\mathbf{f}$ are the inputs and outputs.

Assumption 3 The weight matrices $\mathbf{W}$, $\mathbf{V}$ satisfy $\|\mathbf{W}\|_{\mathrm{F}} \le W_{\max}$, $\|\mathbf{V}\|_{\mathrm{F}} \le V_{\max}$, where $W_{\max}$ and $V_{\max}$ are positive constants.

2.4 Control objective

The control objective is to design control laws for thrust force $\mathbf{T}$, torque $\boldsymbol{\tau}$ and update laws for $\mathbf{W}$, $\mathbf{V}$, so that the underactuated underwater vehicle is able to track a given reference trajectory $\boldsymbol{\eta}_{\mathrm{d}}(t)$ and the position error $\|\boldsymbol{\eta}_1 - \boldsymbol{\eta}_{\mathrm{d}}(t)\|$ converges to a neighborhood of the origin that can be made arbitrarily small.

Assumption 4 The reference trajectory $\boldsymbol{\eta}_{\mathrm{d}}(t)$ is sufficiently smooth and its derivatives are bounded, given as

$$\|\dot{\boldsymbol{\eta}}_{\mathrm{d}}(t)\| \le \xi_1,\ \|\ddot{\boldsymbol{\eta}}_{\mathrm{d}}(t)\| \le \xi_2,\ \|\boldsymbol{\eta}_{\mathrm{d}}^{(3)}(t)\| \le \xi_3,\ \|\boldsymbol{\eta}_{\mathrm{d}}^{(4)}(t)\| \le \xi_4$$

where ξ_1, ξ_2, ξ_3, ξ_4 are all positive constants.

Remark 1 For a specific vehicle, due to the limitation of the vehicle's physical structure, the vehicle cannot track any faster trajectories. That's why we set boundedness for the reference's derivatives in Assumption 4.

3 Multilayer NNs-based controller

This section describes the design of a multilayer NN-based tracking controller for an underactuated AUV. The multilayer NNs are resorted to estimate the lumped unmodeled dynamics and time-varying disturbances, where projections are applied to ensure the estimated weights to be bounded. Figure 3 illustrates the main blocks of the control system.

3.1 Controller design

Step 1 We first define the position tracking error in the body-fixed frame as

$$\mathbf{e}_1 = \mathbf{J}(\boldsymbol{\eta}_2)^\top (\boldsymbol{\eta}_1 - \boldsymbol{\eta}_d), \tag{8}$$

and an additional error term is given as

$$\mathbf{s} = \dot{\mathbf{e}}_1 + \Lambda \mathbf{e}_1 \tag{9}$$

where Λ is an unknown function that will be specified later, and $\dot{\mathbf{e}}_1$,

$$\dot{\mathbf{e}}_1 = -\mathbf{S}(\boldsymbol{\nu}_2)\mathbf{e}_1 + \boldsymbol{\nu}_1 - \mathbf{J}(\boldsymbol{\eta}_2)^\top \dot{\boldsymbol{\eta}}_{\mathrm{d}}. \tag{10}$$

Inspired by [58], here we want to drive $\mathbf{s}$ to a constant vector $\boldsymbol{\rho} \in \mathbb{R}^3$ instead of zero so as to obtain a continuous controller. Then, we define the second error term as

$$\mathbf{e}_2 = \mathbf{s} - \boldsymbol{\rho} \tag{11}$$

whose time derivative is

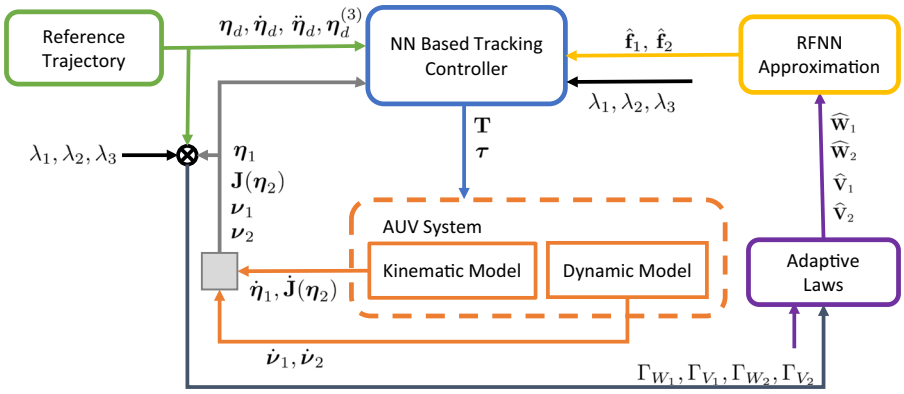

Fig. 3 Block diagram of NNs-based trajectory tracking system

$$\begin{aligned}\dot{\mathbf{e}}_2 = &-\mathbf{S}(\dot{\boldsymbol{\nu}}_2)\mathbf{e}_1 - \mathbf{S}(\boldsymbol{\nu}_2)\dot{\mathbf{e}}_1 + \mathbf{M}^{-1}(-\mathbf{S}(\boldsymbol{\nu}_2)\mathbf{M}\boldsymbol{\nu}_1 + \mathbf{n}_{\nu_1}\mathbf{T}\\ &+ \mathbf{J}(\boldsymbol{\eta}_2)^\top(b - \mathrm{mg})\mathbf{u}_z + \mathbf{d}_{\nu_1}) + \mathbf{S}(\boldsymbol{\nu}_2)\mathbf{J}(\boldsymbol{\eta}_2)^\top\dot{\boldsymbol{\eta}}_\mathrm{d}\\ &- \mathbf{J}(\boldsymbol{\eta}_2)^\top\ddot{\boldsymbol{\eta}}_\mathrm{d} + \dot{\Lambda}\mathbf{e}_1 + \Lambda\dot{\mathbf{e}}_1.\end{aligned} \tag{12}$$

Step 2 In order to obtain the thrust force, the following Lyapunov function is chosen as

$$V_a = \frac{1}{2}\mathbf{e}_1^\top\mathbf{e}_1 + \frac{1}{2}\mathbf{e}_2^\top\mathbf{M}^2\mathbf{e}_2. \tag{13}$$

Taking the time derivative of V_a, one has

$$\begin{aligned}\dot{V}_a = &-\lambda_2\mathbf{e}_2^\top\mathbf{e}_2 + \mathbf{e}_1^\top\boldsymbol{\rho} - \mathbf{e}_1^\top\Lambda\mathbf{e}_1 + \mathbf{e}_2^\top\mathbf{M}\Big(\mathbf{M}^{-1}\mathbf{e}_1\\ &- \mathbf{MS}(\dot{\boldsymbol{\nu}}_2)\mathbf{e}_1 - \mathbf{MS}(\boldsymbol{\nu}_2)\dot{\mathbf{e}}_1\\ &- \mathbf{S}(\boldsymbol{\nu}_2)\mathbf{M}\boldsymbol{\nu}_1 + \mathbf{n}_{\nu_1}\mathbf{T} + \mathbf{J}(\boldsymbol{\eta}_2)^\top(b - \mathrm{mg})\mathbf{u}_z\\ &+ \mathbf{d}_{\nu_1} + \mathbf{MS}(\boldsymbol{\nu}_2)\mathbf{J}(\boldsymbol{\eta}_2)^\top\dot{\boldsymbol{\eta}}_\mathrm{d} - \mathbf{MJ}(\boldsymbol{\eta}_2)^\top\ddot{\boldsymbol{\eta}}_\mathrm{d}\\ &+ \mathbf{M}\dot{\Lambda}\mathbf{e}_1 + \mathbf{M}\Lambda\dot{\mathbf{e}}_1 + \lambda_2\mathbf{M}^{-1}\mathbf{e}_2\Big).\end{aligned} \tag{14}$$

To ensure $(-\mathbf{e}_1^\top\Lambda\mathbf{e}_1)$ is negative definite and eliminate $(-\mathbf{MS}(\dot{\boldsymbol{\nu}}_2)\mathbf{e}_1 - \mathbf{MS}(\boldsymbol{\nu}_2)\dot{\mathbf{e}}_1)$, we choose

$$\Lambda = \mathbf{S}(\boldsymbol{\nu}_2) + \lambda_1\mathbf{M}^{-1} \tag{15}$$

whose time derivative yields

$$\dot{\Lambda} = \mathbf{S}(\dot{\boldsymbol{\nu}}_2) \tag{16}$$

where λ_1 is a positive constant. Substituting (15) and (16) into (14), one obtains

$$\begin{aligned}\dot{V}_a = &-\alpha_1 + \mathbf{e}_1^\top\boldsymbol{\rho} - \mathbf{e}_1^\top\mathbf{S}(\boldsymbol{\nu}_2)\mathbf{e}_1\\ &+ \mathbf{e}_2^\top\mathbf{M}\Big(\mathbf{M}^{-1}\mathbf{e}_1 - \mathbf{MS}(\dot{\boldsymbol{\nu}}_2)\mathbf{e}_1\\ &- \mathbf{MS}(\boldsymbol{\nu}_2)\dot{\mathbf{e}}_1 - \mathbf{S}(\boldsymbol{\nu}_2)\mathbf{M}\boldsymbol{\nu}_1 + \mathbf{n}_{\nu_1}\mathbf{T}\\ &+ \mathbf{J}(\boldsymbol{\eta}_2)^\top(b - \mathrm{mg})\mathbf{u}_z\\ &+ \mathbf{d}_{\nu_1} + \mathbf{MS}(\boldsymbol{\nu}_2)\mathbf{J}(\boldsymbol{\eta}_2)^\top\dot{\boldsymbol{\eta}}_\mathrm{d} - \mathbf{MJ}(\boldsymbol{\eta}_2)^\top\ddot{\boldsymbol{\eta}}_\mathrm{d}\\ &+ \mathbf{MS}(\dot{\boldsymbol{\nu}}_2)\mathbf{e}_1 + \mathbf{M}(\mathbf{S}(\boldsymbol{\nu}_2) + \lambda_1\mathbf{M}^{-1})\dot{\mathbf{e}}_1\\ &+ \lambda_2\mathbf{M}^{-1}\mathbf{e}_2\Big)\end{aligned} \tag{17}$$

which can be simplified as

$$\begin{aligned}\dot{V}_a = &-\alpha_1 + \mathbf{e}_1^\top\boldsymbol{\rho} - \mathbf{e}_1^\top\mathbf{S}(\boldsymbol{\nu}_2)\mathbf{e}_1 + \mathbf{e}_2^\top\mathbf{M}\Big(\mathbf{M}^{-1}\mathbf{e}_1\\ &- \mathbf{S}(\boldsymbol{\nu}_2)\mathbf{M}\boldsymbol{\nu}_1 + \mathbf{n}_{\nu_1}\mathbf{T} + \mathbf{J}(\boldsymbol{\eta}_2)^\top(b - \mathrm{mg})\mathbf{u}_z\\ &+ \mathbf{d}_{\nu_1} + \mathbf{MS}(\boldsymbol{\nu}_2)\mathbf{J}(\boldsymbol{\eta}_2)^\top\dot{\boldsymbol{\eta}}_\mathrm{d} - \mathbf{MJ}(\boldsymbol{\eta}_2)^\top\ddot{\boldsymbol{\eta}}_\mathrm{d}\\ &+ \lambda_1\dot{\mathbf{e}}_1 + \lambda_2\mathbf{M}^{-1}\mathbf{e}_2\Big).\end{aligned} \tag{18}$$

Combining (9) and (15), one gets

$$\boldsymbol{\nu}_1 = \mathbf{e}_2 + \mathbf{J}(\boldsymbol{\eta}_2)^\top\dot{\boldsymbol{\eta}}_\mathrm{d} - \lambda_1\mathbf{M}^{-1}\mathbf{e}_1 + \boldsymbol{\rho}. \tag{19}$$

Substituting (10), (19) into (18), $\dot{V}_a$ becomes

$$\begin{aligned}\dot{V}_a = &-\alpha_1 + \mathbf{e}_1^\top \boldsymbol{\rho} + \mathbf{e}_2^\top \mathbf{M}\Big(- \mathbf{S}(\boldsymbol{v}_2)\mathbf{M}\mathbf{e}_2 \\ &- \mathbf{S}(\boldsymbol{v}_2)\mathbf{M}(\mathbf{J}(\boldsymbol{\eta}_2)^\top \dot{\boldsymbol{\eta}}_{\mathrm{d}} + \boldsymbol{\rho}) + \mathbf{n}_{v_1}\mathbf{T} \\ &+ \mathbf{J}(\boldsymbol{\eta}_2)^\top (b - \mathrm{mg})\mathbf{u}_z + \mathbf{M}\mathbf{S}(\boldsymbol{v}_2)\mathbf{J}(\boldsymbol{\eta}_2)^\top \dot{\boldsymbol{\eta}}_{\mathrm{d}} \\ &- \mathbf{M}\mathbf{J}(\boldsymbol{\eta}_2)^\top \ddot{\boldsymbol{\eta}}_{\mathrm{d}} + \lambda_1(\boldsymbol{v}_1 - \mathbf{J}(\boldsymbol{\eta}_2)^\top \dot{\boldsymbol{\eta}}_{\mathrm{d}}) \\ &+ \lambda_2 \mathbf{M}^{-1}\mathbf{e}_2 + \mathbf{M}^{-1}\mathbf{e}_1 + \mathbf{d}_{v_1}\Big).\end{aligned} \tag{20}$$

It is noted that $\mathbf{e}_2^\top \mathbf{M}\mathbf{S}(\boldsymbol{v}_2)\mathbf{M}\mathbf{e}_2 = 0$, and then it can be obtained that

$$\begin{aligned}\dot{V}_a = &-\alpha_1 + \mathbf{e}_1^\top \boldsymbol{\rho} + \mathbf{e}_2^\top \mathbf{M} \\ &\Big(- \mathbf{S}(\boldsymbol{v}_2)\mathbf{M}(\mathbf{J}(\boldsymbol{\eta}_2)^\top \dot{\boldsymbol{\eta}}_{\mathrm{d}} + \boldsymbol{\rho}) \\ &+ \mathbf{n}_{v_1}\mathbf{T} + \mathbf{J}(\boldsymbol{\eta}_2)^\top (b - \mathrm{mg})\mathbf{u}_z \\ &+ \mathbf{M}\mathbf{S}(\boldsymbol{v}_2)\mathbf{J}(\boldsymbol{\eta}_2)^\top \dot{\boldsymbol{\eta}}_{\mathrm{d}} - \mathbf{M}\mathbf{J}(\boldsymbol{\eta}_2)^\top \ddot{\boldsymbol{\eta}}_{\mathrm{d}} \\ &+ \lambda_1(\boldsymbol{v}_1 - \mathbf{J}(\boldsymbol{\eta}_2)^\top \dot{\boldsymbol{\eta}}_{\mathrm{d}}) + \lambda_2 \mathbf{M}^{-1}\mathbf{e}_2 + \mathbf{M}^{-1}\mathbf{e}_1 + \mathbf{d}_{v_1}\Big),\end{aligned} \tag{21}$$

where $\alpha_1 = \lambda_1 \mathbf{e}_1^\top \mathbf{M}^{-1}\mathbf{e}_1 + \lambda_2 \mathbf{e}_2^\top \mathbf{e}_2$ and λ_2 is a positive number. Let

$$\boldsymbol{\Delta} = \mathbf{S}(\mathbf{M}\boldsymbol{\rho}) + \mathbf{S}(\mathbf{M}\mathbf{J}(\boldsymbol{\eta}_2)^\top \dot{\boldsymbol{\eta}}_{\mathrm{d}}) - \mathbf{M}\mathbf{S}(\mathbf{J}(\boldsymbol{\eta}_2)^\top \dot{\boldsymbol{\eta}}_{\mathrm{d}}),$$

then $\dot{V}_a$ can be reorganized as

$$\begin{aligned}\dot{V}_a = &-\alpha_1 + \mathbf{e}_1^\top \boldsymbol{\rho} + \mathbf{e}_2^\top \mathbf{M}\Big(\boldsymbol{\Theta}\boldsymbol{\varpi} + \mathbf{J}(\boldsymbol{\eta}_2)^\top (b - \mathrm{mg})\mathbf{u}_z \\ &- \mathbf{M}\mathbf{J}(\boldsymbol{\eta}_2)^\top \ddot{\boldsymbol{\eta}}_{\mathrm{d}} \\ &+ \lambda_1(\boldsymbol{v}_1 - \mathbf{J}(\boldsymbol{\eta}_2)^\top \dot{\boldsymbol{\eta}}_{\mathrm{d}}) + \lambda_2 \mathbf{M}^{-1}\mathbf{e}_2 + \mathbf{M}^{-1}\mathbf{e}_1 + \mathbf{f}_1\Big)\end{aligned} \tag{22}$$

where $\mathbf{f}_1 = \mathbf{d}_{v_1}$ and

$$\boldsymbol{\Theta} = [\mathbf{n}_{v_1}, \boldsymbol{\Delta}], \quad \boldsymbol{\varpi} = [\mathbf{T}^\top, \boldsymbol{v}_2^\top]^\top. \tag{23}$$

Here, $\boldsymbol{\varpi}$ is regarded as virtual input. It should be noted that $\mathbf{f}_1$ is unknown, and therefore we use multilayer NNs to approximate it, by using the following function:

$$\mathbf{f}_1 = \mathbf{W}_1^\top \sigma(\mathbf{V}_1^\top \mathbf{x}_1) + \boldsymbol{\epsilon}_1(\mathbf{x}_1) \tag{24}$$

where $\mathbf{x}_1 = [1, \boldsymbol{v}_1^\top]^\top \in \mathbb{R}^{4\times 1}$. Correspondingly, the NNs approximation for $\mathbf{f}_1$ is given as

$$\hat{\mathbf{f}}_1 = \widehat{\mathbf{W}}_1^\top \sigma(\widehat{\mathbf{V}}_1^\top \mathbf{x}_1) \tag{25}$$

where $\widehat{\mathbf{W}}_1$ and $\widehat{\mathbf{V}}_1$ are designed estimations of the ideal weight matrix, $\widetilde{\mathbf{W}}_1 = \widehat{\mathbf{W}}_1 - \mathbf{W}_1$, $\widetilde{\mathbf{V}}_1 = \widehat{\mathbf{V}}_1 - \mathbf{V}_1$ are the estimation error. However, it is worthy pointing out that because the NNs approximation only holds in a certain compact set. Therefore, if we use the method from (25) directly, global stability cannot be obtained. In light of this consideration and inspired by [51, 59], we introduce

$$\hat{\mathbf{f}}_{n_1} = \vartheta(||\mathbf{x}_1||)\widehat{\mathbf{W}}_1^\top \sigma(\widehat{\mathbf{V}}_1^\top \mathbf{x}_1) + \Big(1 - \vartheta(||\mathbf{x}_1||)\Big)\boldsymbol{\delta}_{n_1} \tag{26}$$

where ς is an arbitrarily small positive constant,

$$\begin{aligned}\boldsymbol{\delta}_{n_1} = \Big[&\zeta_{n_{11}} \tanh\Big(\frac{\mathbf{u}_x^\top \mathbf{M}^\top \mathbf{e}_2 \zeta_{n_{11}}}{\varsigma}\Big), \\ &\zeta_{n_{11}} \tanh\Big(\frac{\mathbf{u}_y^\top \mathbf{M}^\top \mathbf{e}_2 \zeta_{n_{12}}}{\varsigma}\Big), \\ &\zeta_{n_{11}} \tanh\Big(\frac{\mathbf{u}_z^\top \mathbf{M}^\top \mathbf{e}_2 \zeta_{n_{13}}}{\varsigma}\Big)\Big]\end{aligned}$$

and

$$\vartheta(||\mathbf{x}||) = \begin{cases} 1, & ||\mathbf{x}|| \le a_1 \\ \dfrac{\mathrm{e}^{\sigma(||\mathbf{x}||)}}{\mathrm{e}^{||\mathbf{x}||} + \mathrm{e}^{1-\sigma(||\mathbf{x}||)}}, & a_1 < ||\mathbf{x}|| < a_2 \\ 0, & ||\mathbf{x}|| \ge a_2 \end{cases}$$

with $\sigma(||\mathbf{x}||) = -(a_1^2 - a_2^2)(||\mathbf{x}||^2 - a_1^2)^{-1}$, $a_2 > a_1 > 0$, $|\mathbf{u}_x^\top \mathbf{f}_1| \le \zeta_{n_{11}}$, $|\mathbf{u}_y^\top \mathbf{f}_1| \le \zeta_{n_{12}}$, $|\mathbf{u}_z^\top \mathbf{f}_1| \le \zeta_{n_{13}}$, and $\zeta_{n_{11}}$, $\zeta_{n_{12}}$, $\zeta_{n_{13}}$ are known positive numbers.

To obtain the update law for $\widehat{\mathbf{W}}_1$, $\widehat{\mathbf{V}}_1$, the second Lyapunov function is defined as

$$V_b = V_a + \frac{1}{2}\mathrm{tr}(\widetilde{\mathbf{W}}_1^\top \Gamma_{W_1}^{-1}\widetilde{\mathbf{W}}_1) + \frac{1}{2}\mathrm{tr}(\widetilde{\mathbf{V}}_1^\top \Gamma_{V_1}^{-1}\widetilde{\mathbf{V}}_1). \tag{27}$$

Taking the time derivative of V_b, one has

$$\begin{aligned}\dot{V}_b \le &-\alpha_1 + \mathbf{e}_1^\top \boldsymbol{\rho} + \vartheta(||\mathbf{x}_1||)\Big(\mathbf{e}_2^\top \mathbf{M}\boldsymbol{\epsilon}_1(\mathbf{x}_1) - \mathbf{e}_2^\top \mathbf{M}\boldsymbol{\mu}_1\Big) \\ &+ \mathbf{e}_2^\top \mathbf{M}\Big(\boldsymbol{\Theta}\boldsymbol{\varpi} + \mathbf{J}(\boldsymbol{\eta}_2)^\top (b - \mathrm{mg})\mathbf{u}_z - \mathbf{M}\mathbf{J}(\boldsymbol{\eta}_2)^\top \ddot{\boldsymbol{\eta}}_{\mathrm{d}} \\ &+ \lambda_1(\boldsymbol{v}_1 - \mathbf{J}(\boldsymbol{\eta}_2)^\top \dot{\boldsymbol{\eta}}_{\mathrm{d}}) + \lambda_2 \mathbf{M}^{-1}\mathbf{e}_2 \\ &+ \mathbf{M}^{-1}\mathbf{e}_1 + \vartheta(||\mathbf{x}_1||)\widehat{\mathbf{W}}_1^\top \sigma(\widehat{\mathbf{V}}_1^\top \mathbf{x}_1) \\ &+ (1 - \vartheta(||\mathbf{x}_1||))\boldsymbol{\delta}_{n_1}\Big) - \mathbf{e}_2^\top \mathbf{M}\widetilde{\mathbf{W}}_1^\top (\widehat{\sigma}_1 - \widehat{\sigma}_1' \widehat{\mathbf{V}}_1^\top \mathbf{x}_1) \\ &- \mathbf{e}_2^\top \mathbf{M}\widehat{\mathbf{W}}_1^\top \widehat{\sigma}_1' \widetilde{\mathbf{V}}_1^\top \mathbf{x}_1 + \mathrm{tr}(\widetilde{\mathbf{W}}_1^\top \Gamma_{W_1}^{-1}\dot{\widehat{\mathbf{W}}}_1) \\ &+ \mathrm{tr}(\widetilde{\mathbf{V}}_1^\top \Gamma_{V_1}^{-1}\dot{\widehat{\mathbf{V}}}_1) + (1 - \vartheta(||\mathbf{x}_1||))\varsigma_n\end{aligned} \tag{28}$$

where $\boldsymbol{\mu}_1 = \widetilde{\mathbf{W}}_1^\top \widehat{\sigma}_1' \mathbf{V}_1^\top \mathbf{x}_1 - \mathbf{W}_1^\top \mathbf{o}(\widetilde{\mathbf{V}}_1^\top \mathbf{x}_1)^2$, $\widehat{\sigma}_1 = \sigma(\widehat{\mathbf{V}}_1^\top \mathbf{x}_1)$ and $\widehat{\sigma}_1'$ is the partial derivative $\widehat{\sigma}_1' = \partial(\sigma(\widehat{\mathbf{V}}_1^\top \mathbf{x}_1))/\partial(\widehat{\mathbf{V}}_1^\top \mathbf{x}_1)$, $\varsigma_n = 0.2785\varsigma$. Then, the desired virtual input $\boldsymbol{\varpi}_\mathrm{d}$ can be written as

$$\begin{aligned}\boldsymbol{\varpi}_\mathrm{d} = -\mathbf{L}\Big(&\mathbf{J}(\boldsymbol{\eta}_2)^\top (b - \mathrm{mg})\mathbf{u}_z - \mathbf{M}\mathbf{J}(\boldsymbol{\eta}_2)^\top \ddot{\boldsymbol{\eta}}_\mathrm{d} \\ &+ \lambda_1(\boldsymbol{v}_1 - \mathbf{J}(\boldsymbol{\eta}_2)^\top \dot{\boldsymbol{\eta}}_\mathrm{d}) + \lambda_2 \mathbf{M}^{-1}\mathbf{e}_2 + \mathbf{M}^{-1}\mathbf{e}_1 \\ &+ \vartheta(||\mathbf{x}_1||)\widehat{\mathbf{W}}_1^\top \sigma(\widehat{\mathbf{V}}_1^\top \mathbf{x}_1) + (1 - \vartheta(||\mathbf{x}_1||))\boldsymbol{\delta}_{n_1}\Big)\end{aligned} \tag{29}$$

where $\mathbf{L} = \boldsymbol{\Theta}^\top(\boldsymbol{\Theta}\boldsymbol{\Theta}^\top)^{-1}$, with $(\boldsymbol{\Theta}\boldsymbol{\Theta}^\top)$ being invertible by choosing $\boldsymbol{\rho}$ properly [58].

It can be further obtained the control law for thrust force

$$\mathbf{T} = \mathbf{h}_1 \boldsymbol{\varpi}_\mathrm{d}, \tag{30}$$

the desired angular velocity

$$\boldsymbol{v}_{2d} = \mathbf{h}_2 \boldsymbol{\varpi}_\mathrm{d}, \tag{31}$$

and the update laws for $\widehat{\mathbf{W}}_1$, $\widehat{\mathbf{V}}_1$

$$\begin{aligned}\dot{\widehat{\mathbf{W}}}_1 &= \Gamma_{W_1}\vartheta(||\mathbf{x}_1||)(\widehat{\sigma}_1 - \widehat{\sigma}_1'\widehat{\mathbf{V}}_1^\top \mathbf{x}_1)\mathbf{e}_2^\top \mathbf{M} \\ \dot{\widehat{\mathbf{V}}}_1 &= \Gamma_{V_1}\vartheta(||\mathbf{x}_1||)\mathbf{x}_1 \mathbf{e}_2^\top \mathbf{M}\widehat{\mathbf{W}}_1^\top \widehat{\sigma}_1'\end{aligned} \tag{32}$$

where $\mathbf{h}_1 = [\mathbf{1}_{2\times 2}, \mathbf{0}_{2\times 3}]$, $\mathbf{h}_2 = [\mathbf{0}_{3\times 2}\, \mathbf{1}_{3\times 3}]$; Γ_{W_1} and Γ_{V_1} are positive definite, diagonal matrices.

In order to avoid estimation drift and ensure $\|\widehat{\mathbf{W}}_1\|_\mathrm{F}^2 \le W_{m1}$, $W_{m1} > 0$, we design the update laws for $\widehat{\mathbf{W}}_1$ by using a projection modified from [60], given by

$$\dot{\widehat{\mathbf{W}}}_1 = \begin{cases} \Gamma_{W_1}\mathbf{z}_1\mathbf{e}_2^\top \mathbf{M}, & \text{if } \mathrm{tr}(\widehat{\mathbf{W}}_1^\top \widehat{\mathbf{W}}_1) < W_{m1} \\ & \text{or } \mathrm{tr}(\widehat{\mathbf{W}}_1^\top \widehat{\mathbf{W}}_1) = W_{m1} \text{ and } \mathbf{e}_2^\top \mathbf{M}\widehat{\mathbf{W}}_1^\top \mathbf{z}_1 < 0 \\ \Gamma_{W_1}\mathbf{z}_1\mathbf{e}_2^\top \mathbf{M} - \Gamma_{W_1}\dfrac{\mathbf{e}_2^\top \mathbf{M}\widehat{\mathbf{W}}_1^\top \mathbf{z}_1}{\mathrm{tr}(\widehat{\mathbf{W}}_1^\top \widehat{\mathbf{W}}_1)}\widehat{\mathbf{W}}_1 & \\ \text{if } \mathrm{tr}(\widehat{\mathbf{W}}_1^\top \widehat{\mathbf{W}}_1) = W_{m1} \text{ and } \mathbf{e}_2^\top \mathbf{M}\widehat{\mathbf{W}}_1^\top \mathbf{z}_1 \ge 0 & \end{cases} \tag{33}$$

where $\mathbf{z}_1 = \vartheta(||\mathbf{x}_1||)(\widehat{\sigma}_1 - \widehat{\sigma}_1'\widehat{\mathbf{V}}_1^\top \mathbf{x}_1)$. Similarly, it is guaranteed that $\|\widehat{\mathbf{V}}_1\|_\mathrm{F}^2 \le V_{m1}$, $V_{m1} > 0$ by rewriting the update law for $\mathbf{V}_1$ as

$$\dot{\widehat{\mathbf{V}}}_1 = \begin{cases} \Gamma_{V_1}\mathbf{x}_1\mathbf{z}_2, & \text{if } \mathrm{tr}(\widehat{\mathbf{V}}_1^\top \widehat{\mathbf{V}}_1) < V_{m1} \text{ or } \mathrm{tr}(\widehat{\mathbf{V}}_1^\top \widehat{\mathbf{V}}_1) \\ & = V_{m1} \text{ and } \mathbf{z}_2\widehat{\mathbf{V}}_1^\top \mathbf{x}_1 < 0 \\ \Gamma_{V_1}\mathbf{x}_1\mathbf{z}_2 - \Gamma_{V_1}\dfrac{\mathbf{z}_2\widehat{\mathbf{V}}_1^\top \mathbf{x}_1}{\mathrm{tr}(\widehat{\mathbf{V}}_1^\top \widehat{\mathbf{V}}_1)}\widehat{\mathbf{V}}_1, & \text{if } \mathrm{tr}(\widehat{\mathbf{V}}_1^\top \widehat{\mathbf{V}}_1) \\ & = V_{m1} \text{ and } \mathbf{z}_2\widehat{\mathbf{V}}_1^\top \mathbf{x}_1 \ge 0 \end{cases} \tag{34}$$

where $\mathbf{z}_2 = \vartheta(||\mathbf{x}_1||)(\mathbf{e}_2^\top \mathbf{M}\widehat{\mathbf{W}}_1^\top \widehat{\sigma}_1')$.

Step 3 Now, we introduce the third tracking error as

$$\mathbf{e}_3 = \boldsymbol{v}_2 - \boldsymbol{v}_{2d}. \tag{35}$$

Substituting (30), (33), (34) and (35) into (28), one obtains

$$\begin{aligned}\dot{V}_b \le &-\alpha_1 + \mathbf{e}_1^\top \boldsymbol{\rho} + \vartheta(||\mathbf{x}_1||) \\ &\Big(\mathbf{e}_2^\top \mathbf{M}\boldsymbol{\epsilon}_1(\mathbf{x}_1) - \mathbf{e}_2^\top \mathbf{M}\boldsymbol{\mu}_1\Big) \\ &+ \mathbf{e}_2^\top \mathbf{M}\boldsymbol{\Theta}\mathbf{h}_2^\top \mathbf{e}_3 + (1 - \vartheta(||\mathbf{x}_1||))\varsigma_n.\end{aligned} \tag{36}$$

Consider the following Lyapunov function with $\mathbf{e}_3$ as

$$V_c = V_b + \frac{1}{2}\mathbf{e}_3^\top \mathbf{I}\mathbf{e}_3. \tag{37}$$

The time derivative of V_c is

$$\begin{aligned}\dot{V}_c \le &-\alpha_2 + \mathbf{e}_1^\top \boldsymbol{\rho} + \vartheta(||\mathbf{x}_1||) \\ &\Big(\mathbf{e}_2^\top \mathbf{M}\boldsymbol{\epsilon}_1(\mathbf{x}_1) - \mathbf{e}_2^\top \mathbf{M}\boldsymbol{\mu}_1\Big) + \mathbf{e}_3^\top(\boldsymbol{\tau} + \mathbf{d}_{v_2} \\ &- \mathbf{I}\mathbf{h}_2\dot{\boldsymbol{\varpi}}_\mathrm{d} + \lambda_3\mathbf{e}_3 + \mathbf{h}_2\boldsymbol{\Theta}^\top \mathbf{M}^\top \mathbf{e}_2) \\ &+ (1 - \vartheta(||\mathbf{x}_1||))\varsigma_n,\end{aligned} \tag{38}$$

where $\alpha_2 = \alpha_1 + \lambda_3\mathbf{e}_3^\top \mathbf{e}_3$, the expression of $\dot{\boldsymbol{\varpi}}_\mathrm{d}$ is given as

$$\begin{aligned}\dot{\boldsymbol{\varpi}}_\mathrm{d} = -\dot{\mathbf{L}}\Big(&\mathbf{J}(\boldsymbol{\eta}_2)^\top (b - \mathrm{mg})\mathbf{u}_z - \mathbf{M}\mathbf{J}(\boldsymbol{\eta}_2)^\top \ddot{\boldsymbol{\eta}}_\mathrm{d} \\ &+ \lambda_1(\boldsymbol{v}_1 - \mathbf{J}(\boldsymbol{\eta}_2)^\top \dot{\boldsymbol{\eta}}_\mathrm{d}) + \lambda_2\mathbf{M}^{-1}\mathbf{e}_2 \\ &+ \mathbf{M}^{-1}\mathbf{e}_1 + \widehat{\mathbf{W}}_1^\top \sigma(\widehat{\mathbf{V}}_1^\top \mathbf{x}_1)\Big) \\ &- \mathbf{L}\Big(-\mathbf{S}(\boldsymbol{v}_2)\mathbf{J}(\boldsymbol{\eta}_2)^\top (b - \mathrm{mg})\mathbf{u}_z \\ &+ \mathbf{M}\mathbf{S}(\boldsymbol{v}_2)\mathbf{J}(\boldsymbol{\eta}_2)^\top \ddot{\boldsymbol{\eta}}_\mathrm{d} - \mathbf{M}\mathbf{J}(\boldsymbol{\eta}_2)^\top \boldsymbol{\eta}_\mathrm{d}^{(3)} \\ &+ \lambda_1\mathbf{S}(\boldsymbol{v}_2)\mathbf{J}(\boldsymbol{\eta}_2)^\top \dot{\boldsymbol{\eta}}_\mathrm{d} \\ &- \lambda_1\mathbf{J}(\boldsymbol{\eta}_2)^\top \ddot{\boldsymbol{\eta}}_\mathrm{d} + \mathbf{M}^{-1}\dot{\mathbf{e}}_1 \\ &+ \vartheta(||\mathbf{x}_1||)\dot{\widehat{\mathbf{W}}}_1^\top \sigma(\widehat{\mathbf{V}}_1^\top \mathbf{x}_1) + \boldsymbol{\beta}\Big)\end{aligned} \tag{39}$$

where

$$\begin{aligned}\boldsymbol{\beta} = {} & \lambda_2 \mathbf{M}^{-1}\dot{\mathbf{e}}_2 + \lambda_1 \dot{\boldsymbol{\nu}}_1 + \dot{\vartheta}(||\mathbf{x}_1||)\widehat{\mathbf{W}}_1^{\top}\sigma(\widehat{\mathbf{V}}_1^{\top}\mathbf{x}_1) \\ & + \vartheta(||\mathbf{x}_1||)\widehat{\mathbf{W}}_1^{\top}\dot{\sigma}(\widehat{\mathbf{V}}_1^{\top}\mathbf{x}_1) \\ & - \dot{\vartheta}(||\mathbf{x}_1||)\boldsymbol{\delta}_{n_1} + (1-\vartheta(||\mathbf{x}_1||))\dot{\boldsymbol{\delta}}_{n_1}\end{aligned} \tag{40}$$

contains unknown term $\mathbf{d}_{\nu_1}$. For simplicity, we firstly remove the unknown term from $\dot{\boldsymbol{\nu}}_1$ and define

$$\begin{aligned}\bar{\dot{\boldsymbol{\nu}}}_1 = {} & -\mathbf{M}^{-1}\mathbf{S}(\boldsymbol{\nu}_2)\mathbf{M}\boldsymbol{\nu}_1 + \mathbf{M}^{-1}\mathbf{n}_{\nu_1}\mathbf{T} \\ & + \mathbf{M}^{-1}\mathbf{J}(\boldsymbol{\eta}_2)^{\top}(b-\mathrm{mg})\mathbf{u}_z.\end{aligned} \tag{41}$$

Then, $\boldsymbol{\beta}$ can be rewritten as $\boldsymbol{\beta} = \bar{\boldsymbol{\beta}} + \partial\boldsymbol{\beta}/\partial\boldsymbol{\nu}_1\mathbf{d}_{\nu_1}$, and all terms in $\bar{\boldsymbol{\beta}}$ are known.

Substituting (39) into (38), $\dot{V}_c$ becomes

$$\begin{aligned}\dot{V}_c \le {} & -\alpha_2 + \mathbf{e}_1^{\top}\boldsymbol{\rho} + \vartheta(||\mathbf{x}_1||)(\mathbf{e}_2^{\top}\mathbf{M}\boldsymbol{\epsilon}_1(\mathbf{x}_1) \\ & - \mathbf{e}_2^{\top}\mathbf{M}\boldsymbol{\mu}_1) + \mathbf{e}_3^{\top}\Big(\boldsymbol{\tau} + \lambda_3\mathbf{e}_3 + \mathbf{h}_2\boldsymbol{\Theta}^{\top}\mathbf{M}^{\top}\mathbf{e}_2 \\ & - \mathbf{I}\mathbf{h}_2(\dot{\bar{\boldsymbol{\varpi}}}_{\mathrm{d}} - \mathbf{L}\dot{\bar{\boldsymbol{\beta}}}) + \mathbf{f}_2\Big) + (1-\vartheta(||\mathbf{x}_1||))\varsigma_n,\end{aligned} \tag{42}$$

where $\bar{\boldsymbol{\varpi}}_{\mathrm{d}} = \dot{\boldsymbol{\varpi}}_{\mathrm{d}} + \mathbf{L}\boldsymbol{\beta}$ and

$$\mathbf{f}_2 = \mathbf{d}_{\nu_2} + \mathbf{I}\mathbf{h}_2\mathbf{L}(\partial\boldsymbol{\beta}/\partial\boldsymbol{\nu}_1)\mathbf{d}_{\nu_1}. \tag{43}$$

Note that $\mathbf{f}_2$ includes unknown terms $\mathbf{d}_{\nu_1}$ and $\mathbf{d}_{\nu_2}$; similarly, we use multilayer NNs to estimate $\mathbf{f}_2$, given by

$$\mathbf{f}_2 = \mathbf{W}_2^{\top}\sigma(\mathbf{V}_2^{\top}\mathbf{x}_2) + \boldsymbol{\epsilon}_2(\mathbf{x}_2) \tag{44}$$

where

$$\begin{aligned}\mathbf{x}_2 = {} & [1,\ \hat{w}_{11},\ \ldots,\hat{w}_{43},\ (\partial\sigma(\boldsymbol{\nu}_1)/\partial\boldsymbol{\nu}_1)^{\top},\ \boldsymbol{\nu}_1^{\top},\ \boldsymbol{\nu}_2^{\top}, \\ & (\mathbf{J}(\boldsymbol{\eta}_2)^{\top}\dot{\boldsymbol{\eta}}_{\mathrm{d}})^{\top}]^{\top} \in \mathbb{R}^{25\times 1}.\end{aligned}$$

The NNs approximation for $\mathbf{f}_2$ is given as

$$\hat{\mathbf{f}}_2 = \widehat{\mathbf{W}}_2^{\top}\sigma(\widehat{\mathbf{V}}_2^{\top}\mathbf{x}_2) \tag{45}$$

where $\widehat{\mathbf{W}}_2$, $\widehat{\mathbf{V}}_2$ and $\widetilde{\mathbf{W}}_2 = \widehat{\mathbf{W}}_2 - \mathbf{W}_2$, $\widetilde{\mathbf{V}}_2 = \widehat{\mathbf{V}}_2 - \mathbf{V}_2$ represent the estimation of the ideal weight matrices and estimation errors, respectively. To achieve global stability, similar to the definition of (26), $\hat{\mathbf{f}}_{n_2}$ is introduced as

$$\hat{\mathbf{f}}_{n_2} = \vartheta(||\mathbf{x}_2||)\widehat{\mathbf{W}}_2^{\top}\sigma(\widehat{\mathbf{V}}_2^{\top}\mathbf{x}_2) + \Big(1-\vartheta(||\mathbf{x}_2||)\Big)\boldsymbol{\delta}_{n_2} \tag{46}$$

where

$$\begin{aligned}\boldsymbol{\delta}_{n_2} = {} & \Big[\zeta_{n_{21}}\tanh\Big(\frac{\mathbf{u}_x^{\top}\mathbf{e}_3\zeta_{n_{21}}}{\varsigma}\Big),\ \zeta_{n_{21}} \\ & \tanh\Big(\frac{\mathbf{u}_y^{\top}\mathbf{e}_3\zeta_{n_{22}}}{\varsigma}\Big), \zeta_{n_{21}}\tanh\Big(\frac{\mathbf{u}_z^{\top}\mathbf{e}_3\zeta_{n_{23}}}{\varsigma}\Big)\Big]\end{aligned}$$

and $|\mathbf{u}_x^{\top}\mathbf{f}_2| \le \zeta_{n_{21}}$, $|\mathbf{u}_y^{\top}\mathbf{f}_2| \le \zeta_{n_{22}}$, $|\mathbf{u}_z^{\top}\mathbf{f}_2| \le \zeta_{n_{23}}$, and $\zeta_{n_{21}}$, $\zeta_{n_{22}}$, $\zeta_{n_{23}}$ are known positive numbers.

Define the last control Lyapunov function as

$$V_{\mathrm{d}} = V_c + \frac{1}{2}\mathrm{tr}(\widetilde{\mathbf{W}}_2^{\top}\Gamma_{W_2}^{-1}\widetilde{\mathbf{W}}_2) + \frac{1}{2}\mathrm{tr}(\widetilde{\mathbf{V}}_2^{\top}\Gamma_{V_2}^{-1}\widetilde{\mathbf{V}}_2). \tag{47}$$

Taking the derivative of V_{d} with respect to time t, it can be obtained that

$$\begin{aligned}\dot{V}_{\mathrm{d}} \le {} & -\alpha_2 + \mathbf{e}_1^{\top}\boldsymbol{\rho} + \vartheta(||\mathbf{x}_1||)\Big(\mathbf{e}_2^{\top}\mathbf{M}\boldsymbol{\epsilon}_1(\mathbf{x}_1) - \mathbf{e}_2^{\top}\mathbf{M}\boldsymbol{\mu}_1\Big) \\ & + \vartheta(||\mathbf{x}_2||)\Big(\mathbf{e}_3^{\top}\boldsymbol{\epsilon}_2(\mathbf{x}_2) - \mathbf{e}_3^{\top}\boldsymbol{\mu}_2\Big) + \mathbf{e}_3^{\top}\Big(\boldsymbol{\tau} + \lambda_3\mathbf{e}_3 \\ & + \mathbf{h}_2\boldsymbol{\Theta}^{\top}\mathbf{M}^{\top}\mathbf{e}_2 + \vartheta(||\mathbf{x}_2||)\widehat{\mathbf{W}}_2^{\top}\sigma(\widehat{\mathbf{V}}_2^{\top}\mathbf{x}_2) \\ & + \Big(1-\vartheta(||\mathbf{x}_2||)\Big)\boldsymbol{\delta}_{n_2} - \mathbf{I}\mathbf{h}_2(\dot{\bar{\boldsymbol{\varpi}}}_{\mathrm{d}} - \mathbf{L}\dot{\bar{\boldsymbol{\beta}}})\Big) \\ & - \mathbf{e}_3^{\top}\widehat{\mathbf{W}}_2^{\top}(\hat{\sigma}_2 - \hat{\sigma}_2'\widehat{\mathbf{V}}_2^{\top}\mathbf{x}_2) + \mathrm{tr}(\widetilde{\mathbf{W}}_2^{\top}\Gamma_{W_2}^{-1}\dot{\widehat{\mathbf{W}}}_2) \\ & - \mathbf{e}_3^{\top}\widehat{\mathbf{W}}_2^{\top}\hat{\sigma}_2'\widetilde{\mathbf{V}}_2^{\top}\mathbf{x}_2 + \mathrm{tr}(\widetilde{\mathbf{V}}_2^{\top}\Gamma_{V_2}^{-1}\dot{\widehat{\mathbf{V}}}_2) \\ & + (1-\vartheta(||\mathbf{x}_1||))\varsigma_n + (1-\vartheta(||\mathbf{x}_2||))\varsigma_n.\end{aligned} \tag{48}$$

where $\boldsymbol{\mu}_2 = \widetilde{\mathbf{W}}_2^{\top}\hat{\sigma}_2'\mathbf{V}_2^{\top}\mathbf{x}_2 - \mathbf{W}_2^{\top}\mathbf{o}(\widetilde{\mathbf{V}}_2^{\top}\mathbf{x}_2)^2$, $\hat{\sigma}_2 = \sigma(\widehat{\mathbf{V}}_2^{\top}\mathbf{x}_2)$ and $\hat{\sigma}_2'$ is the partial derivative $\hat{\sigma}_2' = \partial(\sigma(\widehat{\mathbf{V}}_2^{\top}\mathbf{x}_2))/\partial(\widehat{\mathbf{V}}_2^{\top}\mathbf{x}_2)$. Choose the last control law, torque, as

$$\begin{aligned}\boldsymbol{\tau} = {} & -(\lambda_3\mathbf{e}_3 + \mathbf{h}_2\boldsymbol{\Theta}^{\top}\mathbf{M}^{\top}\mathbf{e}_2 + \widehat{\mathbf{W}}_2^{\top}\sigma(\widehat{\mathbf{V}}_2^{\top}\mathbf{x}_2) \\ & + \mathbf{I}\mathbf{h}_2(\dot{\bar{\boldsymbol{\varpi}}}_{\mathrm{d}} - \mathbf{L}\dot{\bar{\boldsymbol{\beta}}}))\end{aligned} \tag{49}$$

the update law for $\widehat{\mathbf{W}}_2$

$$\dot{\widehat{\mathbf{W}}}_2 = \begin{cases} \Gamma_{W_2}\mathbf{z}_3\mathbf{e}_3^{\top}, & \text{if } \mathrm{tr}(\widehat{\mathbf{W}}_2^{\top}\widehat{\mathbf{W}}_2) < W_{m2} \\ & \text{or } \mathrm{tr}(\widehat{\mathbf{W}}_2^{\top}\widehat{\mathbf{W}}_2) = W_{m2} \text{ and } \mathbf{e}_3^{\top}\widehat{\mathbf{W}}_2^{\top}\mathbf{z}_3 < 0 \\ \Gamma_{W_2}\mathbf{z}_3\mathbf{e}_3^{\top} - \Gamma_{W_2}\dfrac{\mathbf{e}_3^{\top}\widehat{\mathbf{W}}_2^{\top}\mathbf{z}_3}{\mathrm{tr}(\widehat{\mathbf{W}}_2^{\top}\widehat{\mathbf{W}}_2)}\widehat{\mathbf{W}}_2 & \\ \text{if } \mathrm{tr}(\widehat{\mathbf{W}}_2^{\top}\widehat{\mathbf{W}}_2) = W_{m2} \text{ and } \mathbf{e}_3^{\top}\widehat{\mathbf{W}}_2^{\top}\mathbf{z}_3 \ge 0 & \end{cases} \tag{50}$$

where $W_{m2} > 0$, $\mathbf{z}_3 = \vartheta(||\mathbf{x}_2||)(\hat{\sigma}_2 - \hat{\sigma}_2'\widehat{\mathbf{V}}_2^{\top}\mathbf{x}_2)$. And the update law for $\widehat{\mathbf{V}}_2$

$$\dot{\widehat{\mathbf{V}}}_2 = \begin{cases} \Gamma_{V_2}\mathbf{x}_2\mathbf{z}_4, & \text{if } \mathrm{tr}(\widehat{\mathbf{V}}_2^\top\widehat{\mathbf{V}}_2) < V_{m2} \\ & \text{or } \mathrm{tr}(\widehat{\mathbf{V}}_2^\top\widehat{\mathbf{V}}_2) = V_{m2} \text{ and } \mathbf{z}_4\widehat{\mathbf{V}}_2^\top\mathbf{x}_2 < 0 \\ \Gamma_{V_2}\mathbf{x}_2\mathbf{z}_4 - \Gamma_{V_2}\dfrac{\mathbf{z}_4\widehat{\mathbf{V}}_2^\top\mathbf{x}_2}{\mathrm{tr}(\widehat{\mathbf{V}}_2^\top\widehat{\mathbf{V}}_2)}\widehat{\mathbf{V}}_2, & \\ \text{if } \mathrm{tr}(\widehat{\mathbf{V}}_2^\top\widehat{\mathbf{V}}_2) = V_{m2} \text{ and } \mathbf{z}_4\widehat{\mathbf{V}}_2^\top\mathbf{x}_2 \geq 0 & \end{cases} \tag{51}$$

where $V_{m2} > 0$, $\mathbf{z}_4 = \vartheta(||\mathbf{x}_2||)\mathbf{e}_3^\top\widehat{\mathbf{W}}_2^\top\widehat{\sigma}_2'$. Substituting (49), (50), (51) to (48), one gets

$$\begin{aligned} \dot{V}_\mathrm{d} \leq & -\alpha_2 + \mathbf{e}_1^\top\boldsymbol{\rho} + \vartheta(||\mathbf{x}_1||)\mathbf{e}_2^\top(\mathbf{M}\boldsymbol{\epsilon}_1(\mathbf{x}_1) - \mathbf{M}\boldsymbol{\mu}_1) \\ & + \vartheta(||\mathbf{x}_2||)\mathbf{e}_3^\top(\boldsymbol{\epsilon}_2(\mathbf{x}_2) - \boldsymbol{\mu}_2) + (1 - \vartheta(||\mathbf{x}_1||))\varsigma_n \\ & + (1 - \vartheta(||\mathbf{x}_2||))\varsigma_n. \end{aligned} \tag{52}$$

Theorem 1 *For an underactuated autonomous vehicle modeled by* (1), (4), *through designing control laws* (30), (49) *and update laws* (33), (34), (50), (51), *the vehicle is able to track a smooth reference trajectory in the presence of unmodeled dynamic terms and time-varying disturbances and error terms* $\mathbf{e}_1, \mathbf{e}_2, \mathbf{e}_3$ *converge to an arbitrarily small tube centered at the origin. Consequently, global uniformly ultimately bounded is achieved. Meanwhile, the estimated* $\widehat{\mathbf{W}}_1, \widehat{\mathbf{W}}_2, \widehat{\mathbf{V}}_1, \widehat{\mathbf{V}}_2$ *are guaranteed to be bounded and satisfying*

$$\begin{aligned} \mathrm{tr}(\widehat{\mathbf{W}}_1^\top\widehat{\mathbf{W}}_1) \leq W_{m1}, \mathrm{tr}(\widehat{\mathbf{V}}_1^\top\widehat{\mathbf{V}}_1) \leq V_{m1}, \mathrm{tr}(\widehat{\mathbf{W}}_2^\top\widehat{\mathbf{W}}_2) \\ \leq W_{m2}, \mathrm{tr}(\widehat{\mathbf{V}}_2^\top\widehat{\mathbf{V}}_2) \leq V_{m2}, \end{aligned}$$

where W_{m1}, V_{m1}, W_{m2}, V_{m2} are positive numbers.

Proof The proof is presented in the "Appendix." □

3.2 Extended controller with measurement noises

To simulate the actual operation scenario, we take the measurement noises into consideration. White noise is added to the position $\boldsymbol{\eta}_1$, linear velocity $\boldsymbol{\nu}_1$ and angular velocity $\boldsymbol{\nu}_2$ of the AUV. To suppress the measurement noises' harmful effects, we let $\boldsymbol{\eta}_1, \boldsymbol{\nu}_1, \boldsymbol{\nu}_2$ pass through a second-order linear tracking differentiator [61, 62] to obtain an estimation of these values as follows:

$$\begin{cases} \dot{\boldsymbol{\eta}}_{1f} = \boldsymbol{\eta}_{1m} \\ \dot{\boldsymbol{\eta}}_{1m} = -k_{\eta_1}^2(\boldsymbol{\eta}_{1f} - \boldsymbol{\eta}_1) - 2k_{\eta_1}\boldsymbol{\eta}_{1m} \end{cases} \tag{53}$$

$$\begin{cases} \dot{\boldsymbol{\nu}}_{1f} = \boldsymbol{\nu}_{1m} \\ \dot{\boldsymbol{\nu}}_{1m} = -k_{\nu_1}^2(\boldsymbol{\nu}_{1f} - \boldsymbol{\nu}_1) - 2k_{\nu_1}\boldsymbol{\nu}_{1m} \end{cases} \tag{54}$$

$$\begin{cases} \dot{\boldsymbol{\nu}}_{2f} = \boldsymbol{\nu}_{2m} \\ \dot{\boldsymbol{\nu}}_{2m} = -k_{\nu_2}^2(\boldsymbol{\nu}_{2f} - \boldsymbol{\nu}_2) - 2k_{\nu_2}\boldsymbol{\nu}_{2m} \end{cases} \tag{55}$$

where $k_{\eta_1}, k_{\nu_1}, k_{\nu_2} > 0$, $\boldsymbol{\eta}_{1f}$, $\boldsymbol{\nu}_{1f}$, $\boldsymbol{\nu}_{2f}$ are the filtered position, linear velocity and angular velocity.

Remark 2 As stated by [62], the tracking differentiator (53), (54), (55) assures that the state arrives at the steady state in a finite time T. Namely, there exist constants η_{1i}^*, ν_{1i}^*, ν_{2i}^*, such that $|\eta_{1i} - \eta_{1mi}| \leq \eta_{1i}^*$, $|\nu_{1i} - \nu_{1mi}| \leq \nu_{1i}^*$, $|\nu_{2i} - \nu_{2mi}| \leq \nu_{2i}^*$, $i = 1, 2, 3$.

4 Numerical examples

Numerical examples are presented in this section to demonstrate the robustness and effectiveness of the proposed controller. In the presence of unmodeled dynamic terms and external time-varying disturbances, the multilayer NNs-based controller is simulated and compared with the single-layer NNs-based controller.

4.1 Vehicle parameters setting

Referring from [63], physical parameters of the AUV are configured as $m = 54.54\,\mathrm{kg}$, $b = 53.4\,\mathrm{N}$, $X_{\dot{u}} = -7.6e-3$, $Y_{\dot{v}} = -5.5e-2$, $Z_{\dot{w}} = -2.4e-1$, $I_x = 13.58$, $I_y = 20.38$, $I_z = 13.587$, $L_{\dot{p}} = -1e-3$, $M_{\dot{q}} = -1.7e-2$, $N_{\dot{r}} = -3.4e-3$. The unknown terms $\mathbf{d}_{\nu_1} = [d_{\nu_{11}}, d_{\nu_{12}}, d_{\nu_{13}}]^\top$, $\mathbf{d}_{\nu_2} = [d_{\nu_{21}}, d_{\nu_{22}}, d_{\nu_{23}}]^\top$ are chosen randomly and assumed to be very large. The detailed expressions are given in Table 2, with $w_1 = 0.05$, $w_2 = 0.03$, $v_{11} = \mathbf{u}_x^\top\boldsymbol{\nu}_1$, $v_{12} = \mathbf{u}_y^\top\boldsymbol{\nu}_1$, $v_{13} = \mathbf{u}_z^\top\boldsymbol{\nu}_1$, $v_{21} = \mathbf{u}_x^\top\boldsymbol{\nu}_2$, $v_{22} = \mathbf{u}_y^\top\boldsymbol{\nu}_2$ and $v_{23} = \mathbf{u}_z^\top\boldsymbol{\nu}_2$. The reference trajectory is chosen as

$$\boldsymbol{\eta}_\mathrm{d} = [30\cos(\pi/300t),\ 30\sin(\pi/300t),\ 0.02t]^\top\ (\mathrm{m}).$$

4.2 Control parameters setting

Control parameters include control gains (λ_1, λ_2, λ_3), estimation gains (Γ_{W_1}, Γ_{V_1}, Γ_{W_2}, Γ_{V_2}) and neuron numbers. To obtain desirable tracking and estimation

Table 2 Unmodeled terms and external disturbances for an underwater vehicle

Symbol	Expression
$d_{v_{11}}$	$10(v_{11}+v_{11}v_{12}+2v_{12}v_{13})+5(\cos(w_1t)+\sin(w_2t))$
$d_{v_{12}}$	$10(v_{11}v_{12}+v_{12}+2v_{13})+10\sin(w_1t)\cos(w_2t)$
$d_{v_{13}}$	$10(2v_{12}v_{13}+v_{11}v_{12}v_{13})+2\cos(w_1t)+8\sin(w_1t)$
$d_{v_{21}}$	$5(v_{11}v_{23}+v_{11}v_{21}+v_{21}v_{22}+2v_{13}v_{23})+5\cos(w_2t)+2.5\sin(w_1t)$
$d_{v_{22}}$	$5(2v_{11}v_{12}v_{21}+v_{12}v_{22}+v_{13}v_{23})+5\sin(w_2t)\cos(w_1t)+2.5\sin(w_2t)$
$d_{v_{23}}$	$5(2v_{11}v_{22}+v_{12}v_{21}+v_{13}v_{23})+7.5\sin(w_2t)+2.5\cos(w_1t)$

Table 3 Ultimate bounds and root-mean-square errors (RMSEs) of error terms obtained from the proposed control method and the controller with single-layer NNs with smaller (SLNN-S) and larger estimation gains (SLNN-L)

Methods	Ultimate bounds			RMSE		
	$\|\mathbf{e}_1\|$	$\|\mathbf{e}_2\|$	$\|\mathbf{e}_3\|$	$\|\mathbf{e}_1\|$	$\|\mathbf{e}_2\|$	$\|\mathbf{e}_3\|$
Proposed method	0.0852	0.0034	0.0115	0.0845	0.0024	0.0045
SLNN-L	0.1095	0.1150	0.0197	0.0894	0.0796	0.0107
SLNN-S	0.1893	0.3704	0.1200	0.1254	0.2516	0.0728

performance, we need to choose them properly. Theoretically, larger control gains will increase the convergence rate and reduce the ultimate tracking errors. However, larger λ_1, λ_2, λ_3 will lead to more chattering which is an undesirable property from a practical view. For estimation gains and neuron numbers, the theoretical tuning guideline is to (i) use constant estimation gains, but increase the number of neurons until the estimation performance will not be improved anymore; (ii) increase the values of estimation gains to enhance the learning rate. Nonetheless, too many neurons will cost large computational burden and too large Γ_{W_1}, Γ_{V_1}, Γ_{W_2}, Γ_{V_2} could cause instability [49]. Consequently, we need to find a trade-off between the robustness and ultimate trajectory tracking accuracy.

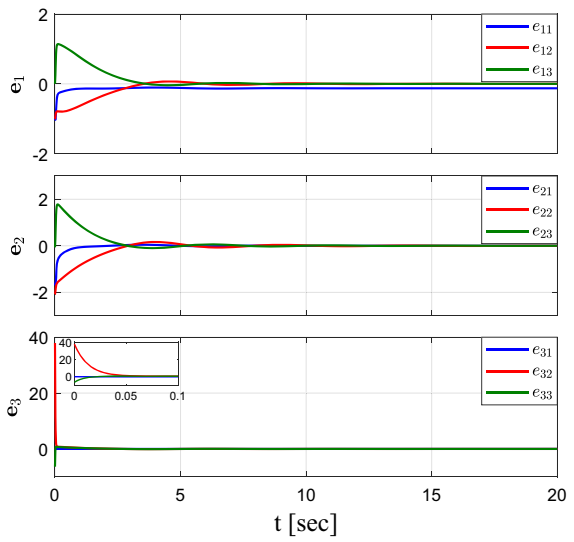

Fig. 4 Tracking errors $\mathbf{e}_1$, $\mathbf{e}_2$, $\mathbf{e}_3$ of the multilayer NNs-based controller

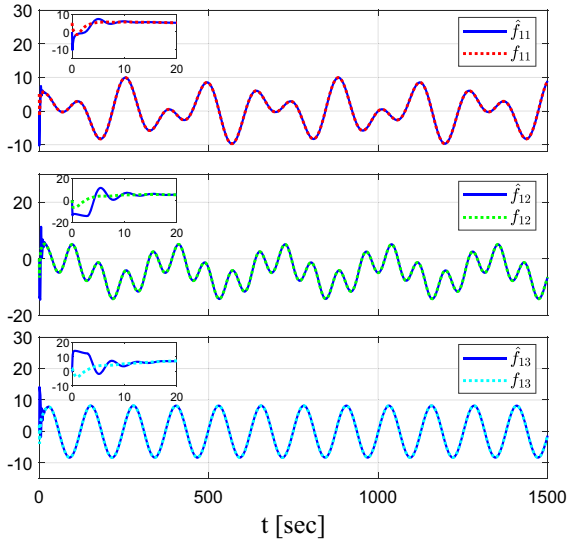

Fig. 5 Unknown term $\mathbf{f}_1 = [f_{11}, f_{12}, f_{13}]^\top$ and its estimation $\hat{\mathbf{f}}_1 = [\hat{f_{11}}, \hat{f_{12}}, \hat{f_{13}}]^\top$

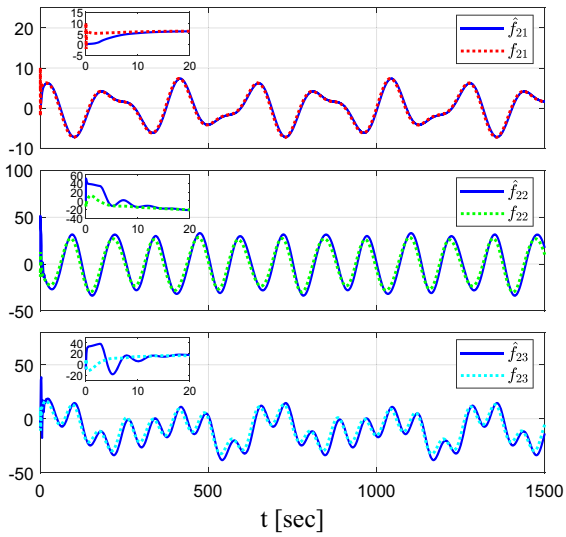

Fig. 6 Unknown term $\mathbf{f}_2 = [f_{21}, f_{22}, f_{23}]^\top$ and its estimation $\hat{\mathbf{f}}_2 = [\hat{f_{21}}, \hat{f_{22}}, \hat{f_{23}}]^\top$

4.3 Simulation results without measurement noises

4.3.1 Trajectory tracking results

Figure 4 further shows the specific tracking errors $\mathbf{e}_1$, $\mathbf{e}_2$, $\mathbf{e}_3$, where we can see that all of these errors converge to the neighborhood of zeros after some fluctuation at the beginning. To directly display the disturbance suppression ability, the approximation of unknown terms and disturbances is shown in Figs. 5 and 6. Both of the estimated uncertainties $\hat{\mathbf{f}}_1$ and $\hat{\mathbf{f}}_2$ converge to the neighborhood of their corresponding desired real functions denoted by $\mathbf{f}_1$ and $\mathbf{f}_2$, respectively. To further demonstrate that the vehicle can converge to the reference trajectory with larger initial position errors, Figs. 7 and 8 are presented. It is obtained that the proposed method is able to steer the vehicle moving along the reference trajectory closely

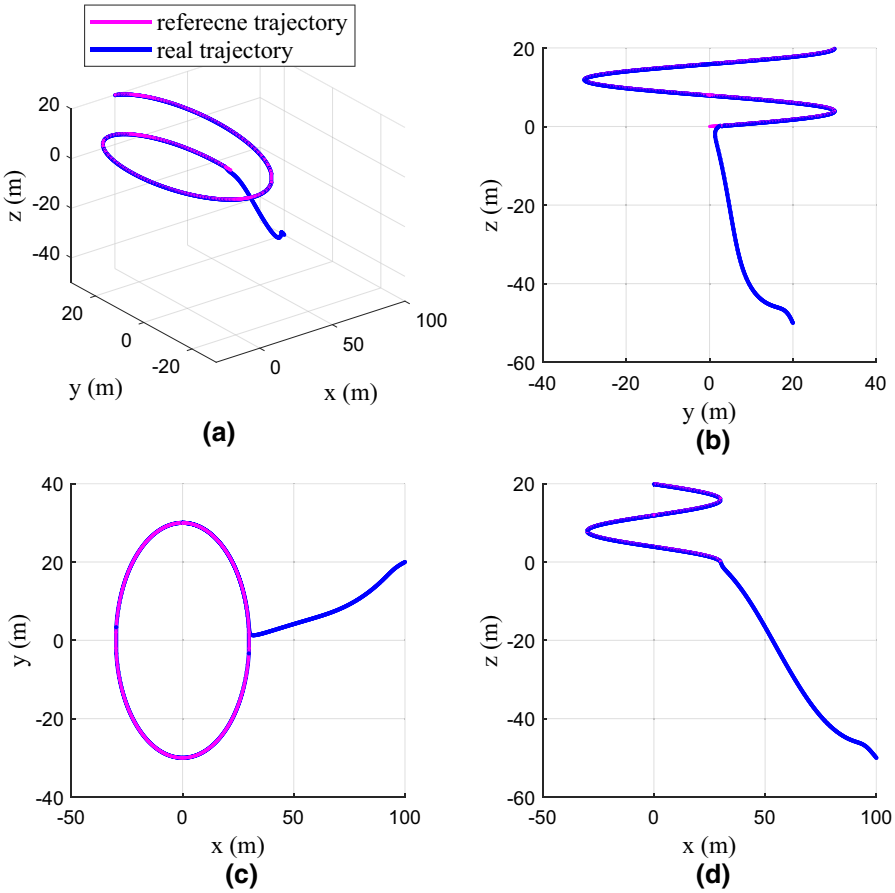

Fig. 7 Reference and real trajectories of an AUV with initial positions $[0, 30, 0]^\top$ (m) and $[100, 20, -50]^\top$ (m), respectively, in **a** 3D, **b** *yz* plane, **c** *xy* plane, and **d** *xz* plane

with initial positions $[100, 20, -50]^\top$ (m) and $[50, -70, -35]^\top$ (m).

4.3.2 Comparison results

To validate the performance of the proposed multi-layer NNs-based controller, we compare it with the single-layer NNs-based tracking controller. Figures 9 and 10 present the tracking error terms, and their corresponding ultimate bounds (UBs) and root-mean-square errors (RMSEs) are given in Table 3. It concludes that (i) larger estimation gains can help to improve the final estimation performance, validated by the result that the UBs and RMSEs of the error terms are obtained from the single-layer NNs-based controller. It is found that larger estimation gains are smaller than those obtained from the single-layer NNs-based controller with smaller estimation gains; (ii) larger estimation gains could cause undesired instability or oscillation. As shown in Fig. 10, the angular velocity error $||\mathbf{e}_3||$ is obtained from the single-layer NNs-based controller with larger estimation gains; at around $t = 1$ [s], unwanted peaks appear; (iii) the proposed controller achieves smoother convergence with smaller UBs and RMSEs.

4.4 Simulation results with measurement noises

To simulate the real operation scenarios, we add white noises to $\boldsymbol{\eta}_1$, $\boldsymbol{v}_1$ and $\boldsymbol{v}_2$. Letting them pass through filters defined by (53), (54), (55), cleaner states are obtained and shown in Figs. 11, 12 and 13. The filtered states denoted by the dashed lines in these diagrams are smoother. Furthermore, Fig. 14 gives the tracking errors $\mathbf{e}_1$, $\mathbf{e}_2$, $\mathbf{e}_3$, from which we can see that all these errors converge to the neighborhood of zero.

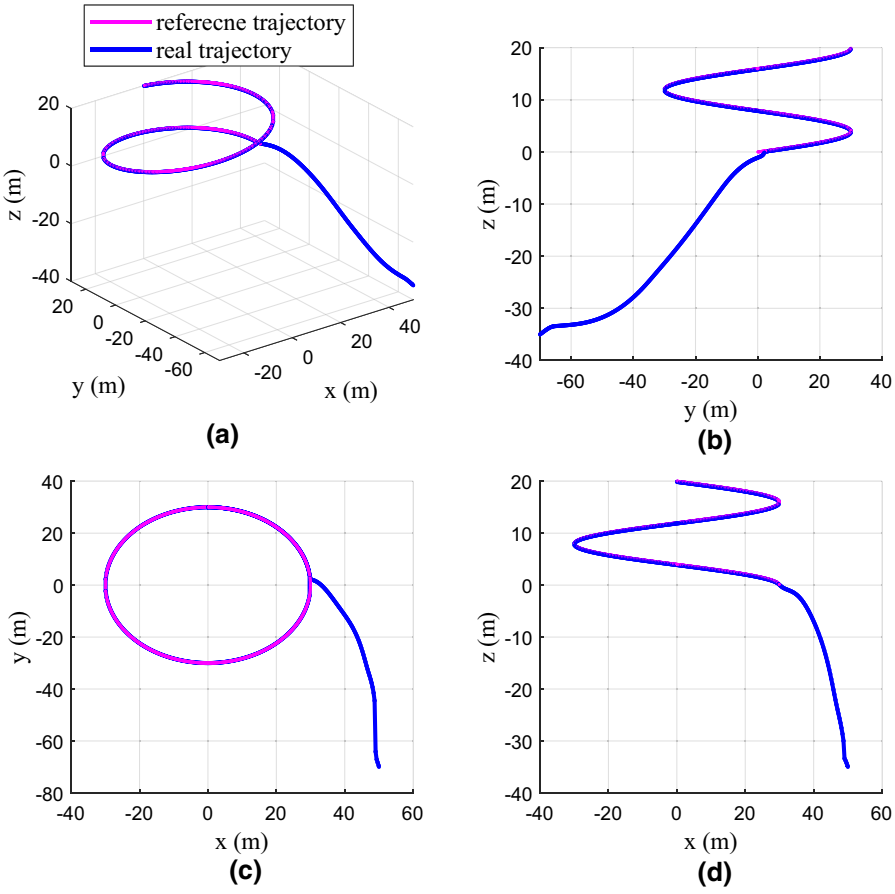

Fig. 8 Reference and real trajectories of an AUV with initial positions $[0, 30, 0]^\top$ (m) and $[50, -70, -35]^\top$ (m), respectively, in **a** 3D, **b** *yz* plane, **c** *xy* plane, and **d** *xz* plane

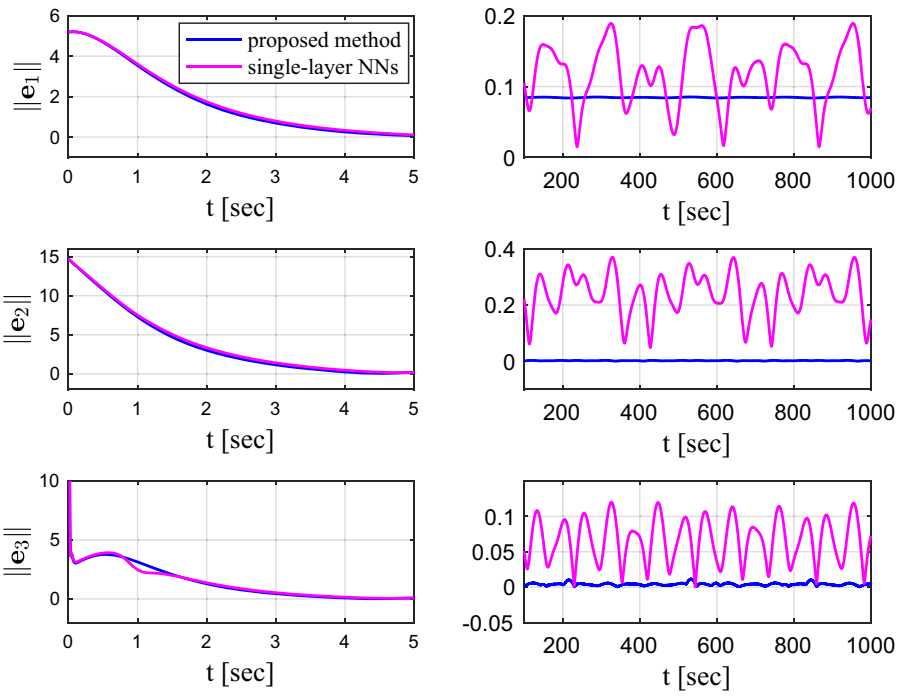

Fig. 9 The norm of tracking errors obtained from the proposed control method and the controller with single-layer NNs (with smaller estimation gains)

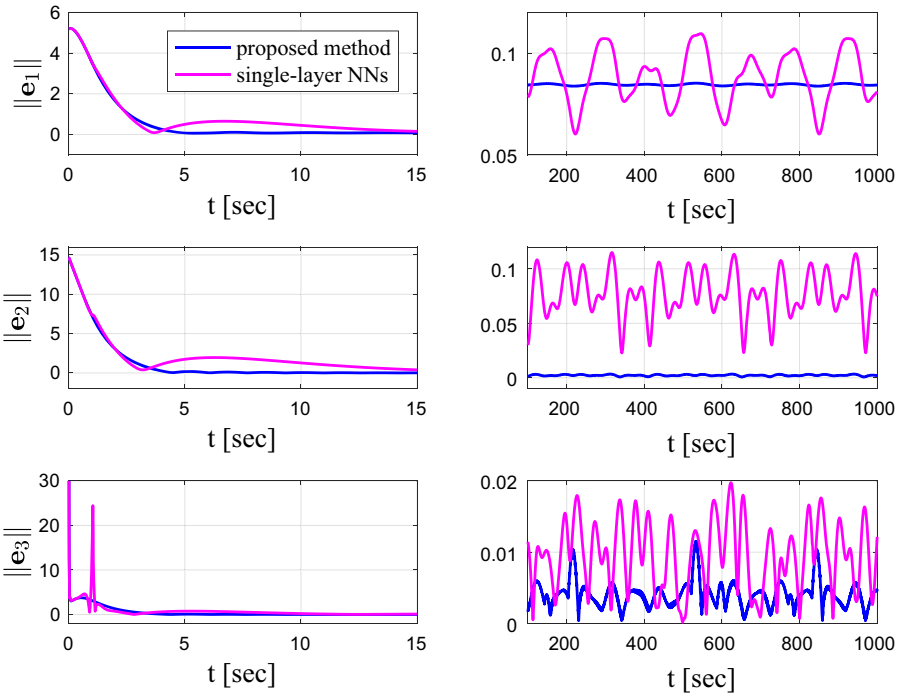

Fig. 10 The norm of tracking errors obtained from the proposed control method and the controller with single-layer NNs (with larger estimation gains)

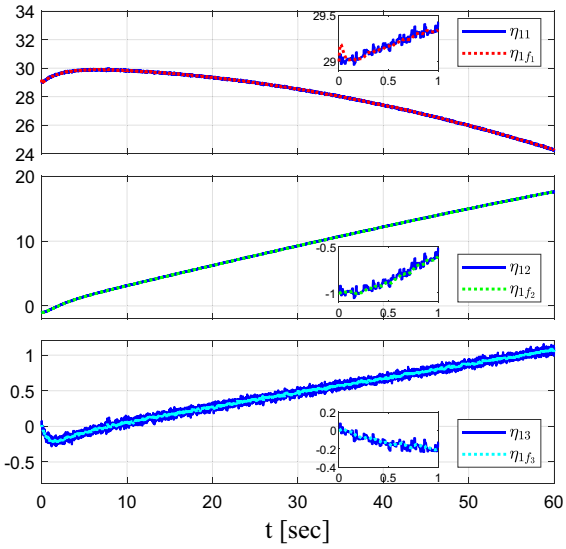

Fig. 11 The positions with noises $\boldsymbol{\eta}_1 = [\eta_{11}, \eta_{12}, \eta_{13}]^\top$ and filtered positions $\boldsymbol{\eta}_{1f} = [\eta_{1f_1}, \eta_{1f_2}, \eta_{1f_3}]^\top$

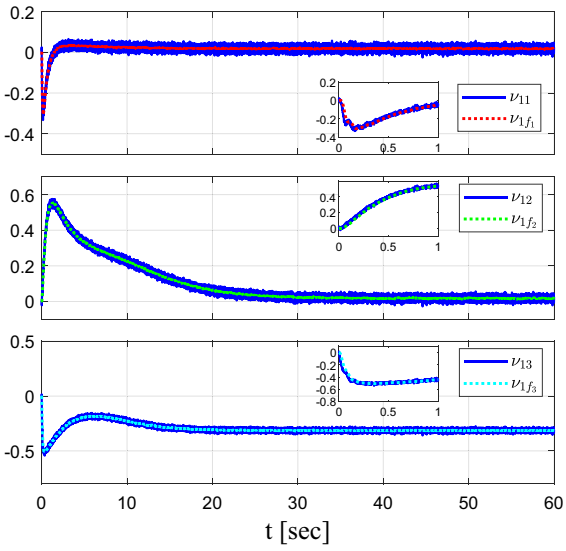

Fig. 12 The linear velocity with white noises $\boldsymbol{\nu}_1 = [\nu_{11}, \nu_{12}, \nu_{13}]^\top$ and filtered linear velocity $\boldsymbol{\nu}_{1f} = [\nu_{1f_1}, \nu_{1f_2}, \nu_{1f_3}]^\top$

5 Conclusion

In this paper, a solution is proposed to solve the problem of trajectory tracking for an underactuated underwater vehicle in the presence of unmodeled dynamic terms and external time-varying disturbances. To obtain robust performance, we use multilayer NNs to approximate the unmodeled dynamic terms and disturbances. The application of smooth projectors ensures that the estimated weights are bounded. As a consequence, global uniformly ultimately bounded is achieved and verified via Lyapunov stability criteria and simulation results.

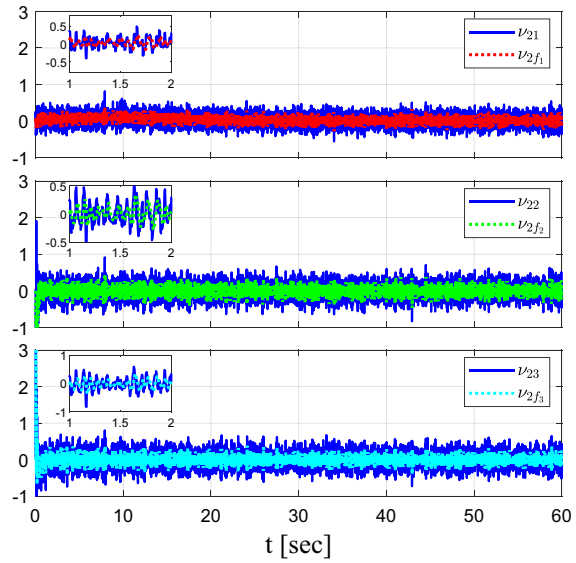

Fig. 13 The angular velocity with white noise $\boldsymbol{\nu}_2 = [\nu_{21}, \nu_{22}, \nu_{23}]^\top$ and filtered angular velocity $\boldsymbol{\nu}_{2f} = [\nu_{2f_1}, \nu_{2f_2}, \nu_{2f_3}]^\top$

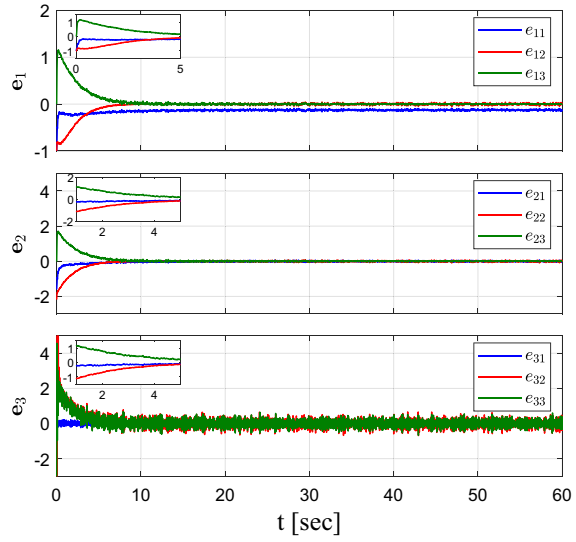

Fig. 14 The tracking errors $\mathbf{e}_1$, $\mathbf{e}_2$, $\mathbf{e}_3$ with white noises and filters

One of our future directions is to take unavailable states into consideration when deriving the control laws. Another future work is to extend the control method to other types of autonomous vehicles such as surface or aerial vehicle.

Funding This study was funded by the following research grants: (1) Nature-Inspired Computing and Metaheuristics Algorithms for Optimizing Data Mining Performance, Grant No. MYRG2016-00069-FST, by the University of Macau; and (2) A Scalable Data Stream Mining Methodology: Stream-based Holistic Analytics and Reasoning in Parallel, Grant No. FDCT/126/2014/A3, by FDCT Macau; and 2018 Guangzhou Science and Technology Innovation and Development of Special Funds, (3) Grant No. EF003/FST-FSJ/2019/GSTIC, and (4) EF004/FST-FSJ/2019/GSTIC.

Compliance with ethical standards

Conflict of interest The authors declare that they have no conflict of interest.

Appendix

Proof of Theorem 1 Rewrite $\dot{V}_\mathrm{d}$ as

$$\begin{aligned}\dot{V}_\mathrm{d} \le & -\lambda_1 \mathbf{e}_1^\top \mathbf{M}^{-1}\mathbf{e}_1 - \lambda_2 \mathbf{e}_2^\top \mathbf{e}_2 - \lambda_3 \mathbf{e}_3^\top \mathbf{e}_3 \\ & + \mathbf{e}_1^\top \boldsymbol{\rho} + \vartheta(||\mathbf{x}_1||)\mathbf{e}_2^\top \Big(\mathbf{M}\boldsymbol{\epsilon}_1(\mathbf{x}_1) - \mathbf{M}\boldsymbol{\mu}_1\Big) \\ & + \vartheta(||\mathbf{x}_2||)\mathbf{e}_3^\top(\boldsymbol{\epsilon}_2(\mathbf{x}_2) - \boldsymbol{\mu}_2) + a\end{aligned} \tag{56}$$

where $a = 2\varsigma_n$ is an arbitrarily small positive constant, and

$$\begin{aligned}\boldsymbol{\mu}_1 &= \widetilde{\mathbf{W}}_1^\top \widehat{\sigma}_1' \mathbf{V}_1^\top \mathbf{x}_1 - \mathbf{W}_1^\top \mathbf{o}(\widetilde{\mathbf{V}}_1^\top \mathbf{x}_1)^2, \\ \boldsymbol{\mu}_2 &= \widetilde{\mathbf{W}}_2^\top \widehat{\sigma}_2' \mathbf{V}_2^\top \mathbf{x}_2 - \mathbf{W}_2^\top \mathbf{o}(\widetilde{\mathbf{V}}_2^\top \mathbf{x}_2)^2,\end{aligned}$$

and

$$\begin{aligned}\mathbf{x}_1 &= [1, \boldsymbol{v}_1^\top]^\top, \\ \mathbf{x}_2 &= [1, \hat{w}_{11}, \ldots, \hat{w}_{43}, (\partial\sigma(\boldsymbol{v}_1)/\partial \boldsymbol{v}_1)^\top, \\ &\quad \boldsymbol{v}_1^\top, \boldsymbol{v}_2^\top, (\mathbf{J}(\boldsymbol{\eta}_2)^\top \dot{\boldsymbol{\eta}}_\mathrm{d})^\top]^\top.\end{aligned}$$

It is noted that $\boldsymbol{v}_1$ and $\boldsymbol{v}_2$ can be written as

$$\begin{aligned}\boldsymbol{v}_1 &= \mathbf{e}_2 + \mathbf{J}(\boldsymbol{\eta}_2)^\top \dot{\boldsymbol{\eta}}_\mathrm{d} - \lambda_1 \mathbf{M}^{-1}\mathbf{e}_1 + \boldsymbol{\rho}, \\ \boldsymbol{v}_2 &= \mathbf{e}_3 + \mathbf{h}_2 \boldsymbol{\varpi}_\mathrm{d}\end{aligned}$$

where $\boldsymbol{\varpi}_\mathrm{d}$ is defined in (29). Inspired by [57], the following facts are introduced, given as, □

Fact 1 For each time t, $\mathbf{x}_1$ is bounded by

$$||\mathbf{x}_1|| \le (a_0 + a_1\xi_1) + a_2||\mathbf{e}_1|| + a_3||\mathbf{e}_2||$$

where a_i, $i = 0, 1, 2, 3$, are computable positive constants.

Fact 2 For each time t, $\mathbf{x}_2$ is bounded by

$$\begin{aligned}||\mathbf{x}_2|| \le & (b_0 + b_1\xi_1 + b_2\xi_2 + b_3 W_\mathrm{max} + b_4\sigma'_\mathrm{max}) \\ & + b_4||\mathbf{e}_1|| + b_5||\mathbf{e}_2|| + b_6||\mathbf{e}_3||\end{aligned}$$

where b_i, $i = 0, 1, \ldots, 6$, are computable positive constants.

Fact 3 For radial basis functions activation functions, the higher-order terms $\mathbf{o}(\widetilde{\mathbf{V}}_1^\top \mathbf{x}_1)^2$ and $\mathbf{o}(\widetilde{\mathbf{V}}_2^\top \mathbf{x}_2)^2$ satisfy the following inequalities:

$$\begin{aligned}\mathbf{o}(\widetilde{\mathbf{V}}_1^\top \mathbf{x}_1)^2 &\le c_{10} + ||\widetilde{\mathbf{V}}_1||_\mathrm{F}(c_{11} + c_{12}||\mathbf{e}_1|| + c_{13}||\mathbf{e}_2||) \\ \mathbf{o}(\widetilde{\mathbf{V}}_2^\top \mathbf{x}_2)^2 &\le c_{20} + ||\widetilde{\mathbf{V}}_2||_\mathrm{F}(c_{21} + c_{22}||\mathbf{e}_1|| \\ &\quad + c_{23}||\mathbf{e}_2|| + c_{24}||\mathbf{e}_3||)\end{aligned}$$

where c_{1i}, c_{2j}, $i = 0, 1, 2, 3$, $j = 0, 1, \ldots, 4$ are computable positive constants.

Fact 4 For $\boldsymbol{\mu}_1$ and $\boldsymbol{\mu}_2$, they satisfy

$$\begin{aligned}||\boldsymbol{\mu}_1|| &\le d_{10} + ||\widetilde{\mathbf{Z}}_1||_\mathrm{F}\Big(d_{11} + d_{12}||\mathbf{e}_1|| + d_{13}||\mathbf{e}_2||\Big) \\ ||\boldsymbol{\mu}_2|| &\le d_{20} + ||\widetilde{\mathbf{Z}}_2||_\mathrm{F}(d_{21} + d_{22}||\mathbf{e}_1|| + d_{23}||\mathbf{e}_2|| + d_{24}||\mathbf{e}_3||)\end{aligned}$$

where d_{1i}, d_{2j}, $i = 0, 1, 2, 3$, $j = 0, 1, \ldots, 4$ are computable positive constants, and $\widetilde{\mathbf{Z}}_1 = \mathrm{diag}(\widetilde{\mathbf{W}}_1, \widetilde{\mathbf{V}}_1)$, $\widetilde{\mathbf{Z}}_2 = \mathrm{diag}(\widetilde{\mathbf{W}}_2, \widetilde{\mathbf{V}}_2)$.

Fact 5 As we have assumed $||\mathbf{W}||_\mathrm{F} \le W_\mathrm{max}$, $||\mathbf{V}||_\mathrm{F} \le V_\mathrm{max}$ and guaranteed $||\hat{\mathbf{W}}_1||_\mathrm{F}^2 \le W_{m1}$, $||\hat{\mathbf{V}}_1||_\mathrm{F}^2 \le V_{m1}$, $||\hat{\mathbf{W}}_2||_\mathrm{F}^2 \le W_{m2}$, $||\hat{\mathbf{V}}_2||_\mathrm{F}^2 \le V_{m2}$, we thereby get the result that

$$||\widetilde{\mathbf{Z}}_1||_\mathrm{F} \le z_{m1},\ ||\widetilde{\mathbf{Z}}_2||_\mathrm{F} \le z_{m2}$$

where z_{m1}, z_{m2} are computable positive constants.

Use the following inequalities:

1. $-\lambda_1 \mathbf{e}_1^\top \mathbf{M}^{-1}\mathbf{e}_1 \le -\lambda_1 \gamma_\mathrm{min}(\mathbf{M}^{-1})||\mathbf{e}_1||^2$
2. $\mathbf{e}_2^\top \mathbf{M}\boldsymbol{\epsilon}_1(\mathbf{x}_1) \le \gamma_\mathrm{max}(\mathbf{M})\Big(\dfrac{||\mathbf{e}_2||^2}{2\varepsilon} + \dfrac{\varepsilon\epsilon_\mathrm{max}^2}{2}\Big)$
3. $\mathbf{e}_1^\top \boldsymbol{\rho} \le \dfrac{||\mathbf{e}_1||^2}{2\varepsilon} + \dfrac{\varepsilon||\boldsymbol{\rho}||^2}{2}$, $\mathbf{e}_3^\top \boldsymbol{\epsilon}_2(\mathbf{x}_2) \le \dfrac{||\mathbf{e}_3||^2}{2\varepsilon} + \dfrac{\varepsilon\epsilon_\mathrm{max}^2}{2}$
4. $-\mathbf{e}_2^\top \mathbf{M}\boldsymbol{\mu}_1 \le \gamma_\mathrm{max}(\mathbf{M})\Big(\dfrac{f_{10}^2}{2\varepsilon} + \dfrac{\varepsilon||\mathbf{e}_2||^2}{2} + \dfrac{f_{11}||\mathbf{e}_1||^2}{2\varepsilon} + \dfrac{f_{11}\varepsilon||\mathbf{e}_2||^2}{2} + f_{12}||\mathbf{e}_2||^2\Big)$

5. $-\mathbf{e}_3^\top \boldsymbol{\mu}_2 \le \frac{f_{20}^2}{2\varepsilon} + \frac{\varepsilon||\mathbf{e}_3||^2}{2} + \frac{f_{21}||\mathbf{e}_1||^2}{2\varepsilon} + \frac{f_{21}\varepsilon||\mathbf{e}_3||^2}{2} + \frac{f_{22}||\mathbf{e}_2||^2}{2\varepsilon} + \frac{f_{22}\varepsilon||\mathbf{e}_3||^2}{2} + f_{23}||\mathbf{e}_3||^2$

where $\gamma_{\min}(\mathbf{M}^{-1})$ and $\gamma_{\max}(\mathbf{M})$ are minimum and maximum eigenvalues of $\mathbf{M}^{-1}$ and $\mathbf{M}$, respectively, $f_{10}, f_{11}, f_{12}, f_{20}, f_{21}, f_{22}, f_{23}$ are computable positive constants, and ε is an arbitrarily small positive constant. Based on these above inequalities, and the facts $0 \le \vartheta(||\mathbf{x}_1||) \le 1$, $0 \le \vartheta(||\mathbf{x}_1||) \le 1$, (56) is rewritten as

$$\begin{aligned}\dot{V}_{\mathrm{d}} \le & -\left(\lambda_1\gamma_{\min}(\mathbf{M}^{-1}) - \frac{1}{2\varepsilon} - \frac{\gamma_{\max}(\mathbf{M})f_{11}}{2\varepsilon} - \frac{f_{11}}{2\varepsilon}\right)||\mathbf{e}_1||^2 \\ & - \left(\lambda_2 - \frac{\gamma_{\max}(\mathbf{M})}{2\varepsilon} - \frac{\gamma_{\max}(\mathbf{M})\varepsilon}{2} \right. \\ & \left. - \frac{\gamma_{\max}(\mathbf{M})f_{11}\varepsilon}{2} - \gamma_{\max}(\mathbf{M})f_{12} - \frac{f_{22}}{2}\right) \\ & ||\mathbf{e}_2||^2 - \left(\lambda_3 - \frac{\varepsilon}{2} - \frac{f_{21}\varepsilon}{2} - \frac{f_{22}\varepsilon}{2} - f_{23}\right)||\mathbf{e}_3||^2 \\ & + \frac{\varepsilon||\boldsymbol{\rho}||^2}{2} + \frac{\gamma_{\max}(\mathbf{M})\epsilon_{\max}^2}{2} + \frac{\varepsilon\epsilon_{\max}^2}{2} + \frac{\gamma_{\max}(\mathbf{M})}{2\varepsilon}f_{10}^2 + \frac{f_{20}^2}{2\varepsilon} \\ = & -\kappa_1\|\mathbf{e}_1\|^2 - \kappa_2\|\mathbf{e}_2\|^2 - \kappa_3\|\mathbf{e}_3\|^2 + \varsigma,\end{aligned} \tag{57}$$

with

$$\begin{aligned}\kappa_1 &= \lambda_1\gamma_{\min}(\mathbf{M}^{-1}) - \frac{1}{2\varepsilon} - \frac{\gamma_{\max}(\mathbf{M})f_{11}}{2\varepsilon} - \frac{f_{11}}{2\varepsilon}, \\ \kappa_2 &= \lambda_2 - \frac{\gamma_{\max}(\mathbf{M})}{2\varepsilon} - \frac{\gamma_{\max}(\mathbf{M})\varepsilon}{2} - \frac{\gamma_{\max}(\mathbf{M})f_{11}\varepsilon}{2} \\ &\quad - \gamma_{\max}(\mathbf{M})f_{12} - \frac{f_{22}}{2}, \\ \kappa_3 &= \lambda_3 - \frac{\varepsilon}{2} - \frac{f_{21}\varepsilon}{2} - \frac{f_{22}\varepsilon}{2} - f_{23}, \\ \varsigma &= \frac{\varepsilon||\boldsymbol{\rho}||^2}{2} + \frac{\gamma_{\max}(\mathbf{M})\epsilon_{\max}^2}{2} + \frac{\varepsilon\epsilon_{\max}^2}{2} \\ &\quad + \frac{\gamma_{\max}(\mathbf{M})}{2\varepsilon}f_{10}^2 + \frac{f_{20}^2}{2\varepsilon}.\end{aligned}$$

By choosing parameters properly, we can guarantee that $\kappa_1, \kappa_2, \kappa_3$ are positive definite. Define $\mathbf{a} = [||\mathbf{e}_1||, ||\mathbf{e}_2||, ||\mathbf{e}_3||]^\top$ and $\kappa_{\min} = \min\{\kappa_1, \kappa_2, \kappa_3\}$; one further can rewrite (57) as

$$\dot{V}_{\mathrm{d}} \le -\kappa_{\min}\mathbf{a}^\top\mathbf{a} + \varsigma \tag{58}$$

which is negative definite for $\|\mathbf{a}\| > \sqrt{\varsigma/\kappa_{\min}}$ which can be made arbitrarily small by adjusting ς and $\kappa_{\min}$.

As a result, global uniformly ultimately bounded is achieved.

At last, inspired by [60], we can prove that the estimated weights $\widehat{\mathbf{W}}_1$, $\widehat{\mathbf{W}}_2$, $\widehat{\mathbf{V}}_1$, $\widehat{\mathbf{V}}_2$ are bounded, and the following inequalities are satisfied:

1. $-\vartheta(||\mathbf{x}_1||)\mathbf{e}_2^\top\mathbf{M}\widetilde{\mathbf{W}}_1^\top(\widehat{\sigma}_1 - \widehat{\sigma}_1'\widehat{\mathbf{V}}_1^\top\mathbf{x}_1) + \mathrm{tr}(\widetilde{\mathbf{W}}_1^\top\Gamma_{W_1}^{-1}\dot{\widehat{\mathbf{W}}}_1) \le 0$
2. $-\vartheta(||\mathbf{x}_1||)\mathbf{e}_2^\top\mathbf{M}\widehat{\mathbf{W}}_1^\top\widehat{\sigma}_1'\widetilde{\mathbf{V}}_1^\top\mathbf{x}_1 + \mathrm{tr}(\widetilde{\mathbf{V}}_1^\top\Gamma_{V_1}^{-1}\dot{\widehat{\mathbf{V}}}_1) \le 0$
3. $-\vartheta(||\mathbf{x}_2||)\mathbf{e}_3^\top\widetilde{\mathbf{W}}_2^\top(\widehat{\sigma}_2 - \widehat{\sigma}_2'\widehat{\mathbf{V}}_2^\top\mathbf{x}_2) + \mathrm{tr}(\widetilde{\mathbf{W}}_2^\top\Gamma_{W_2}^{-1}\dot{\widehat{\mathbf{W}}}_2) \le 0$
4. $-\vartheta(||\mathbf{x}_2||)\mathbf{e}_3^\top\widehat{\mathbf{W}}_2^\top\widehat{\sigma}_2'\widetilde{\mathbf{V}}_2^\top\mathbf{x}_2 + \mathrm{tr}(\widetilde{\mathbf{V}}_2^\top\Gamma_{V_2}^{-1}\dot{\widehat{\mathbf{V}}}_2) \le 0.$

It is noted that due to the above inequalities, the original $\dot{V}_{\mathrm{d}}$

$$\begin{aligned}\dot{V}_{\mathrm{d}} \le & -\lambda_1\mathbf{e}_1^\top\mathbf{M}^{-1}\mathbf{e}_1 - \lambda_2\mathbf{e}_2^\top\mathbf{e}_2 - \lambda_3\mathbf{e}_3^\top\mathbf{e}_3 + \mathbf{e}_1^\top\boldsymbol{\rho} + \vartheta(||\mathbf{x}_1||)\mathbf{e}_2^\top \\ & \left(\mathbf{M}\boldsymbol{\epsilon}_1(\mathbf{x}_1) - \mathbf{M}\boldsymbol{\mu}_1\right) + \vartheta(||\mathbf{x}_2||)\mathbf{e}_3^\top(\boldsymbol{\epsilon}_2(\mathbf{x}_2) - \boldsymbol{\mu}_2) \\ & + a - \vartheta(||\mathbf{x}_1||)\mathbf{e}_2^\top\mathbf{M}\widetilde{\mathbf{W}}_1^\top(\widehat{\sigma}_1 \\ & - \widehat{\sigma}_1'\widehat{\mathbf{V}}_1^\top\mathbf{x}_1) + \mathrm{tr}(\widetilde{\mathbf{W}}_1^\top\Gamma_{W_1}^{-1}\dot{\widehat{\mathbf{W}}}_1) - \vartheta(||\mathbf{x}_1||)\mathbf{e}_2^\top\mathbf{M}\widehat{\mathbf{W}}_1^\top\widehat{\sigma}_1'\widetilde{\mathbf{V}}_1^\top\mathbf{x}_1 \\ & + \mathrm{tr}(\widetilde{\mathbf{V}}_1^\top\Gamma_{V_1}^{-1}\dot{\widehat{\mathbf{V}}}_1) - \vartheta(||\mathbf{x}_2||)\mathbf{e}_3^\top\widetilde{\mathbf{W}}_2^\top(\widehat{\sigma}_2 - \widehat{\sigma}_2'\widehat{\mathbf{V}}_2^\top\mathbf{x}_2) \\ & + \mathrm{tr}(\widetilde{\mathbf{W}}_2^\top\Gamma_{W_2}^{-1}\dot{\widehat{\mathbf{W}}}_2) - \vartheta(||\mathbf{x}_2||)\mathbf{e}_3^\top\widehat{\mathbf{W}}_2^\top\widehat{\sigma}_2'\widetilde{\mathbf{V}}_2^\top\mathbf{x}_2 \\ & + \mathrm{tr}(\widetilde{\mathbf{V}}_2^\top\Gamma_{V_2}^{-1}\dot{\widehat{\mathbf{V}}}_2)\end{aligned} \tag{59}$$

can be rewritten as (56).

References

1. Wang, Y., Wang, R., Wang, S., Tan, M., Yu, J.: Underwater bio-inspired propulsion: from inspection to manipulation. IEEE Trans. Ind. Electron. **67**(9), 7629–7638 (2020)
2. Wu, Z., Liu, J., Yu, J., Fang, H.: Development of a novel robotic dolphin and its application to water quality monitoring. IEEE/ASME Trans. Mechatron. **22**(5), 2130–2140 (2017)
3. Johnson-Roberson, M., Bryson, M., Friedman, A., Pizarro, O., Troni, G., Ozog, P., Henderson, J.C.: High-resolution underwater robotic vision-based mapping and three-dimensional reconstruction for archaeology. J. Field Robot. **34**(4), 625–643 (2017)
4. Hu, H., Song, S., Chen, C.L.P.: Plume tracing via model-free reinforcement learning method. IEEE Trans. Neural Netw. Learn. Syst. **30**(8), 2515–2527 (2019)
5. Wang, N., Qian, C., Sun, J., Liu, Y.: Adaptive robust finite-time trajectory tracking control of fully actuated marine surface vehicles. IEEE Trans. Control Syst. Technol. **24**(4), 1454–1462 (2016)

6. Wang, N., Su, S., Pan, X., Yu, X., Xie, G.: Yaw-guided trajectory tracking control of an asymmetric underactuated surface vehicle. IEEE Trans. Ind. Inform. **15**(6), 3502–3513 (2019)
7. Gao, J., Wu, P., Li, T., Proctor, A.: Optimization-based model reference adaptive control for dynamic positioning of a fully actuated underwater vehicle. Nonlinear Dyn. **87**(4), 2611–2623 (2017)
8. Krupínski, S., Allibert, G., Hua, M., Hamel, T.: An inertial-aided homography-based visual servo control approach for (almost) fully actuated autonomous underwater vehicles. IEEE Trans. Robot. **33**(5), 1041–1060 (2017)
9. Liu, S., Liu, Y., Liang, X., Wang, N.: Uncertainty observation-based adaptive succinct fuzzy-neuro dynamic surface control for trajectory tracking of fully actuated underwater vehicle system with input saturation. Nonlinear Dyn. **98**(3), 1683–1699 (2019)
10. Kim, D.W.: Tracking of remus autonomous underwater vehicles with actuator saturations. Autom. (J. IFAC) **58**(C), 15–21 (2015)
11. von Ellenrieder, K.D.: Dynamic surface control of trajectory tracking marine vehicles with actuator magnitude and rate limits. Automatica **105**, 433–442 (2019)
12. Zheng, Z., Huang, Y., Xie, L., Zhu, B.: Adaptive trajectory tracking control of a fully actuated surface vessel with asymmetrically constrained input and output. IEEE Trans. Control Syst. Technol. **26**(5), 1851–1859 (2018)
13. Li, Y., Wei, C., Wu, Q., Chen, P., Jiang, Y., Li, Y.: Study of 3 dimension trajectory tracking of underactuated autonomous underwater vehicle. Ocean Eng. **105**, 270–274 (2015)
14. Wu, Z., Karimi, H.R., Shi, P.: Practical trajectory tracking of random lagrange systems. Automatica **105**, 314–322 (2019)
15. Liu, Z., Zhang, Y., Yu, X., Yuan, C.: Unmanned surface vehicles: an overview of developments and challenges. Annu. Rev. Control **41**, 71–93 (2016)
16. Martin, S.C., Whitcomb, L.L.: Nonlinear model-based tracking control of underwater vehicles with three degree-of-freedom fully coupled dynamical plant models: theory and experimental evaluation. IEEE Trans. Control Syst. Technol. **26**(2), 404–414 (2018)
17. Li, B., Su, T.C.: Nonlinear heading control of an autonomous underwater vehicle with internal actuators. Ocean Eng. **125**, 103–112 (2016)
18. Shen, C., Shi, Y., Buckham, B.: Trajectory tracking control of an autonomous underwater vehicle using Lyapunov-based model predictive control. IEEE Trans. Ind. Electron. **65**(7), 5796–5805 (2018)
19. Heshmati-Alamdari, S., Karras, G.C., Marantos, P., Kyriakopoulos, K.J.: A robust predictive control approach for underwater robotic vehicles. IEEE Trans. Control Syst. Technol. (2019). https://doi.org/10.1109/TCST.2019.2939248
20. Makavita, C.D., Jayasinghe, S.G., Nguyen, H.D., Ranmuthugala, D.: Experimental study of command governor adaptive control for unmanned underwater vehicles. IEEE Trans. Control Syst. Technol. **27**(1), 332–345 (2019)
21. Rout, R., Subudhi, B.: Narmax self-tuning controller for line-of-sight-based waypoint tracking for an autonomous underwater vehicle. IEEE Trans. Control Syst. Technol. **25**(4), 1529–1536 (2017)
22. Mahapatra, S., Subudhi, B.: Design of a steering control law for an autonomous underwater vehicle using nonlinear h-infinity state feedback technique. Nonlinear Dyn. **90**(2), 837–854 (2017)
23. Elmokadem, T., Zribi, M., Youcef-Toumi, K.: Trajectory tracking sliding mode control of underactuated AUVs. Nonlinear Dyn. **84**(2), 1079–1091 (2016)
24. Jeong, S., Chwa, D.: Coupled multiple sliding-mode control for robust trajectory tracking of hovercraft with external disturbances. IEEE Trans. Ind. Electron. **65**(5), 4103–4113 (2018)
25. Gao, J., An, X., Proctor, A., Bradley, C.: Sliding mode adaptive neural network control for hybrid visual servoing of underwater vehicles. Ocean Eng. **142**, 666–675 (2017)
26. Yu, C., Xiang, X., Wilson, P.A., Zhang, Q.: Guidance-error-based robust fuzzy adaptive control for bottom following of a flight-style AUV with saturated actuator dynamics. IEEE Trans. Cybern. **50**(5), 1887–1899 (2020)
27. Paliotta, C., Lefeber, E., Pettersen, K.Y., Pinto, J., Costa, M., de Figueiredo Borges de Sousa, J.T.: Trajectory tracking and path following for underactuated marine vehicles. IEEE Trans. Control Syst. Technol. **27**(4), 1423–1437 (2019)
28. Wang, N., Er, M.J.: Direct adaptive fuzzy tracking control of marine vehicles with fully unknown parametric dynamics and uncertainties. IEEE Trans. Control Syst. Technol. **24**(5), 1845–1852 (2016)
29. Guo, X., Yan, W., Cui, R.: Event-triggered reinforcement learning-based adaptive tracking control for completely unknown continuous-time nonlinear systems. IEEE Trans. Cybern. 1–12 (2019)
30. Guo, X., Yan, W., Cui, R.: Integral reinforcement learning-based adaptive nn control for continuous-time nonlinear MIMO systems with unknown control directions. IEEE Trans. Syst. Man Cybern. Syst. (2019). https://doi.org/10.1109/TSMC.2019.2897221
31. Cui, R., Yang, C., Li, Y., Sharma, S.: Adaptive neural network control of AUVs with control input nonlinearities using reinforcement learning. IEEE Trans. Syst. Man Cybern. Syst. **47**(6), 1019–1029 (2017)
32. Liu, S., Liu, Y., Wang, N.: Nonlinear disturbance observer-based backstepping finite-time sliding mode tracking control of underwater vehicles with system uncertainties and external disturbances. Nonlinear Dyn. **88**(1), 465–476 (2017)
33. Mu, D., Wang, G., Fan, Y., Qiu, B., Sun, X.: Adaptive course control based on trajectory linearization control for unmanned surface vehicle with unmodeled dynamics and input saturation. Neurocomputing **330**, 1–10 (2019)
34. Bechlioulis, C.P., Karras, G.C., Heshmati-Alamdari, S., Kyriakopoulos, K.J.: Trajectory tracking with prescribed performance for underactuated underwater vehicles under model uncertainties and external disturbances. IEEE Trans. Control Syst. Technol. **25**(2), 429–440 (2017)
35. Yang, X., Yan, J., Hua, C., Guan, X.: Trajectory tracking control of autonomous underwater vehicle with unknown parameters and external disturbances. IEEE Trans. Syst. Man Cybern. Syst. (2019). https://doi.org/10.1109/TSMC.2019.2894171
36. Hamel, T., Samson, C.: Transverse function control of a motorboat. Automatica **65**, 132–139 (2016)

37. Park, B.S.: A simple output-feedback control for trajectory tracking of underactuated surface vessels. Ocean Eng. **143**, 133–139 (2017)
38. Peng, Z., Wang, J.: Output-feedback path-following control of autonomous underwater vehicles based on an extended state observer and projection neural networks. IEEE Trans. Syst. Man Cybern. Syst. **48**(4), 535–544 (2018)
39. Yuan, C., Licht, S., He, H.: Formation learning control of multiple autonomous underwater vehicles with heterogeneous nonlinear uncertain dynamics. IEEE Trans. Cybern. **48**(10), 2920–2934 (2018)
40. Wang, N., Karimi, H.R., Li, H., Su, S.: Accurate trajectory tracking of disturbed surface vehicles: a finite-time control approach. IEEE/ASME Trans. Mechatron. **24**(3), 1064–1074 (2019)
41. Peng, Z., Wang, J., Wang, D.: Distributed maneuvering of autonomous surface vehicles based on neurodynamic optimization and fuzzy approximation. IEEE Trans. Control Syst. Technol. **26**(3), 1083–1090 (2018)
42. Ghavidel, H.F., Kalat, A.A.: Robust control for mimo hybrid dynamical system of underwater vehicles by composite adaptive fuzzy estimation of uncertainties. Nonlinear Dyn. **89**(4), 2347–2365 (2017)
43. Wang, H., Chen, B., Lin, C., Sun, Y., Wang, F.: Adaptive finite-time control for a class of uncertain high-order nonlinear systems based on fuzzy approximation. IET Control Theory Appl. **11**(5), 677–684 (2017)
44. Li, Y., Tong, S., Li, T.: Hybrid fuzzy adaptive output feedback control design for uncertain mimo nonlinear systems with time-varying delays and input saturation. IEEE Trans. Fuzzy Syst. **24**(4), 841–853 (2016)
45. Duan, K., Fong, S., Zhuang, Y., Song, W.: Artificial neural networks in coordinated control of multiple hovercrafts with unmodeled terms. Appl. Sci. **8**(6), 862 (2018)
46. Gao, J., Proctor, A.A., Shi, Y., Bradley, C.: Hierarchical model predictive image-based visual servoing of underwater vehicles with adaptive neural network dynamic control. IEEE Trans. Cybern. **46**(10), 2323–2334 (2016)
47. Shojaei, K.: Neural adaptive robust control of underactuated marine surface vehicles with input saturation. Appl. Ocean Res. **53**, 267–278 (2015)
48. Shojaei, K.: Three-dimensional neural network tracking control of a moving target by underactuated autonomous underwater vehicles. Neural Comput. Appl. **31**(2), 509–521 (2019)
49. Elhaki, O., Shojaei, K.: Neural network-based target tracking control of underactuated autonomous underwater vehicles with a prescribed performance. Ocean Eng. **167**, 239–256 (2018)
50. Elhaki, O., Shojaei, K.: A robust neural network approximation-based prescribed performance output-feedback controller for autonomous underwater vehicles with actuators saturation. Eng. Appl. Artif. Intell. **88**, 103382 (2020)
51. Wang, H., Liu, K., Li, S.: Command filter based globally stable adaptive neural control for cooperative path following of multiple underactuated autonomous underwater vehicles with partial knowledge of the reference speed. Neurocomputing **275**, 1478–1489 (2018)
52. Lin, C., Wang, H., Yuan, J., Yu, D., Li, C.: An improved recurrent neural network for unmanned underwater vehicle online obstacle avoidance. Ocean Eng. **189**, 106327 (2019)
53. Wang, N., Joo Er, M.: Self-constructing adaptive robust fuzzy neural tracking control of surface vehicles with uncertainties and unknown disturbances. IEEE Trans. Control Syst. Technol. **23**(3), 991–1002 (2015)
54. Liu, Y.C., Liu, S.Y., Wang, N.: Fully-tuned fuzzy neural network based robust adaptive tracking control of unmanned underwater vehicle with thruster dynamics. Neurocomputing **196**, 1–13 (2016)
55. Belleter, D., Maghenem, M.A., Paliotta, C., Pettersen, K.Y.: Observer based path following for underactuated marine vessels in the presence of ocean currents: a global approach. Automatica **100**, 123–134 (2019)
56. Fossen, T.I.: Marine control systems: guidance, navigation and control of ships, rigs and underwater vehicles. Marine Cybernetics, Trondheim, Norway (2002)
57. Lewis, F.L., Yesildirek, A., Liu, Kai: Multilayer neural-net robot controller with guaranteed tracking performance. IEEE Trans. Neural Netw. **7**(2), 388–399 (1996)
58. Aguiar, A.P., Hespanha, J.P.: Trajectory-tracking and path-following of underactuated autonomous vehicles with parametric modeling uncertainty. IEEE Trans. Autom. Control **52**(8), 1362–1379 (2007)
59. Tu, L.: An Introduction to Manifolds. Springer, New York (2008)
60. Cheng, L., Hou, Z.G., Tan, M.: Adaptive neural network tracking control for manipulators with uncertain kinematics, dynamics and actuator model. Automatica **45**(10), 2312–2318 (2009)
61. Han, J.: From PID to active disturbance rejection control. IEEE Trans. Ind. Electron. **56**(3), 900–906 (2009)
62. Guo, B.Z., Zhao, Z.L.: On convergence of tracking differentiator. Int. J. Control **84**(4), 693–701 (2011)
63. Karkoub, M., Wu, H.M., Hwang, C.L.: Nonlinear trajectory-tracking control of an autonomous underwater vehicle. Ocean Eng. **145**, 188–198 (2017)